New Astronomy 40 (2015) 87–103

Contents lists available at ScienceDirect

New Astronomy

journal homepage: www.elsevier.com/locate/newast

The nearby Galaxy structure toward the Vela Gum nebula

E.E. Giorgi *,[1], G.R. Solivella [1], G.I. Perren, R.A. Vázquez

Facultad de Ciencias Astronómicas y Geofísicas, UNLP, IALP-CONICET, La Plata, Argentina

HIGHLIGHTS

- The near Galaxy structure in Puppis and Vela has been re-investigated.
- A potential member of the Outer Arm has been recognized by combining photometry and spectroscopy.
- For the first time the parameters of Ruprecht 60 have been computed with UBVI photometry.
- We perform CCD photometry and spectroscopy in five open clusters.

ARTICLE INFO

Article history:
Received 8 October 2014
Received in revised form 31 March 2015
Accepted 4 April 2015
Available online 23 April 2015
Communicated by G.F. Gilmore

Keywords:
Open clusters and associations: general
Milky Way: structure
Galactic spiral arms

ABSTRACT

We report on *UBVI* photometry and spectroscopy for MK classification purposes carried out in the fields of five open clusters projected against the Vela Gum in the Third Galactic Quadrant of the Galaxy. They are Ruprecht 20, Ruprecht 47, Ruprecht 60, NGC 2660 and NGC 2910. We could improve/confirm the parameters of these objects derived before. Ruprecht 20 is not a real physical entity, in agreement with earlier suggestions. Ruprecht 47, a young cluster in the Galactic plane, at 4.4 kpc from the Sun is quite farther than in previous distance estimations and becomes, therefore, a member of the Puppis OB2 association. For the first time Ruprecht 60 was surveyed in *UBVI* photometry. We found it to be placed at 4.2 kpc from the Sun of about and 1 Gyr old. NGC 2660 is another old object in our survey for which distance and age are coincident with previous findings. NGC 2910 turns out to be a young cluster of Vela OB1 association at a distance of 1.4 kpc approximately and 60 Myr old. The spectroscopic parallax method has been applied to several stars located in the fields of four out of the five clusters to get their distances and reddenings. With this method we found two blue stars in the field of NGC 2910 at distances that make them likely members of Vela OB1 too. Also, projected against the fields of Ruprecht 20 and Ruprecht 47 we have detected other young stars favoring not only the existence of Puppis OB1 and OB2 but conforming a young stellar group at ~1 kpc from the Sun and extending for more than 6 kpc outward the Galaxy. If this is the case, there is a thickening of the thin Galactic disk of more than 300 pc at just 2–3 kpc from the Sun. Ruprecht 60 and NGC 2660 are too old objects that have no physical relation with the associations under discussion. An astonishing result has been the detection in the background of Ruprecht 47 of a young star at the impressive distance of 9.5 kpc from the Sun that could be a member of the innermost part of the Outer Arm. Another far young star in the field of NGC 2660, at near 6.0 kpc, may become a probable member of the Perseus Arm or of the inner part of the Local Arm. The distribution of young clusters and stars onto the Third Galactic Quadrant agrees with recent findings concerning the extension of the Local Arm as revealed by parallaxes of regions of star formation. We show evidences too that added to previous ones found by our group explain the thickening of the thin disk as a combination of flare and warp.

1. Introduction

This investigation forms part of a long term project aimed at understanding the nearby spiral structure in the Third Galactic Quadrant of the Milky Way (hereinafter TGQ) from an optical point of view by means of open clusters. The still unresolved question about the grand design structure of the Milky Way (see, e.g. Choi et al. (2014)) has been demanding an extraordinary observational

* Corresponding author.
E-mail addresses: egiorgi@fcaglp.unlp.edu.ar (E.E. Giorgi), gladys@fcaglp.unlp.edu.ar (G.R. Solivella), gperren@fcaglp.unlp.edu.ar (G.I. Perren), rvazquez@fcaglp.unlp.edu.ar (R.A. Vázquez).

[1] Visiting Astronomer, Complejo Astronómico El Leoncito operated under agreement between the Consejo Nacional de Investigaciones Científicas y Técnicas de la República Argentina and the National Universities of La Plata, Córdoba and San Juan.

http://dx.doi.org/10.1016/j.newast.2015.04.004
1384-1076/

effort during the last decades. Actually, a crucial starting point took place in the '70 when Georgelin and Georgelin (1976) produced the first map of the Galaxy utilizing HII regions as spiral tracers. This first map showed that a four arms model fits the observations very well, a concept widely used yet. Since then, a number of other maps showing the structure of the Galaxy have been developed by means of different spiral tracers such as molecular clouds (Efremov, 1998) or by combining them with HII regions (Hou et al., 2009). Dame et al. (2001) collected CO observations from several sources to map the entire Milky Way. While Russeil (2003) carried out a multiwavelength study of the plane of our Galaxy and found evidences that favored a four arms model, Nakanishi and Sofue (1991) presented a three dimensional map constructed with HI observations concluding that a three arms model is better to fit the observations. Churchwell et al. (2009) combined data from a variety of sources in the wavelength range from 3.6 to 24 microns adopting also a four arms model but recognizing some difficulties of interpretation. This is, since the controversy about the number of spiral arms in the Galaxy is still open we suggest the readers to have a look to the summary of spiral arms parameters in the (Vallée, 2013, 2014) paper series and references therein. However, in almost all these cases distances depend on a rotational curve and the adopted kinematic model. Thus, strong ambiguities take place and only can be resolved by adopting other tracers of spiral structures with distances independent from the properties of the models. In this respect, trigonometric parallaxes and proper motions of massive star forming regions in combination with information from HII regions, giant molecular cloud and masers is a promising initiative since distance ambiguities can be removed (Reid et al., 2009, 2014; Hou and Han, 2014). Just to mention, methanol and water masers have been successfully used for some authors to study particular regions of the Milky Way such as the Local, Sagittarius and Perseus Arms (Xu et al. (2013), Wu et al., 2014; Choi et al., 2014, among others).

In this framework, young open clusters become excellent spiral tracers since they can be observed at large distances. The additional advantage of using open clusters is that their distances do not rely on any rotational curve and kinematic model. Contrarily, observations and detection of open clusters are highly dependent of the visual extinction along the line of view in the Galactic plane. Several investigations biased to study the large structure of the Milky Way using open clusters and stellar component were developed by Moffat and Vogt (1973) and Vogt and Moffat (1975) although with a strong magnitude cut-off. This precluded from arriving to conclusive definitions about the extension of the Local Arm (Orion), the angular recognition (and the real entity) of the Perseus Arm and the possible trace of the Outer Arm (Norma-Cygnus). Some other efforts were carried out by McCarthy and Miller (1974), Moffat and FitzGerald (1974), Clariá (1974), Reed and FitzGerald (1984), Reed and FitzGerald (1984), Slawson and Reed (1988), Reed and FitzGerald (1985), Reed (1990), all of them concerning the distribution and structure shown by the stellar components and also by open clusters. Most of the optical inspections performed in the TGQ were concentrated along the region 240° to 280° in longitude, including the Puppis and Vela regions. This could be done, in part, thanks to the presence of a dust-window, the so-called Fitzgerald window (Fitzgerald, 1968) near the Puppis association. A thorough information on related earlier works can be found in Reed (1989) but we also suggest the contribution from Kaltcheva and Hilditch (2000) who revealed the presence of very distant blue stars in the longitude interval from $215^\circ < l < 275^\circ$. Indeed, the absorption has been the greatest obstacle to observations. During the last two decades a notorious feature has been confirmed in the TGQ from the dust mapping for Schlegel et al. (1998) together with the Hydrogen emission maps from SHASSA; these two surveys suggest a symmetry brake-up in the sense that both, dust and emission (neutral gas) show a tendency to locate below the formal Galactic plane at $b = 0^\circ$ Galactic latitude. This fact is in agreement with previous investigations where it has been shown that the HI layer in the Galaxy flares, becomes thicker at larger distances from the Galactic Center (Henderson et al., 1982; Kulkarni et al., 1982; Burton and te Lintel Hekkert, 1986) on a side. On the other, a tendency for the TGQ gas clouds to fall below the Galactic plane has been revealed and interpreted as evidence for warp in the molecular disk as well (May et al., 1988; May et al., 1997). CO observations of the Infrared Astronomical System (IRAS) sources (Wouterloot et al., 1990) concluded that, although the HI layer is substantially thicker than the molecular clouds layer in the inner Galaxy, the z-height distribution of the molecular clouds show the same thickness in the outer Galaxy. A few years ago our group (Vázquez et al., 2008; Carraro et al., 2005; Moitinho et al., 2006; Carraro et al., 2015) presented and discussed a new picture of the spiral structure in the TGQ built by means of a mixture of optical data of open clusters, field blue stars and CO sources distributed along 60 degrees in Galactic longitude. This new picture confirms the presence of the warp (in optical and CO), reveals the existence of the Outer Arm and suggests that the Local Arm extends from the Sun to its encounter with the Outer Arm. However, none of these studies can give definite evidences about the trace of the Perseus Arm except for a very few open clusters that, ambiguously, can be related to the Local Arm too.

Our ongoing observational programme at La Plata Observatory was designed to improve parameters of known clusters and to look for those with no information at all. This is an essential task that allows us to find far spiral tracers and recognize the grand design spiral structure in the TGQ. So, we report here on results coming from CCD *UBVI* photometry combined with spectroscopic measures for five open clusters, Ruprecht 20, Ruprecht 47, Ruprecht 60, NGC 2660 and NGC 2910, all of them projected against the Vela Gum nebula at $240^\circ < l < 260^\circ$ including Vela and Puppis associations. To situate the readers the Gum nebula, one of the biggest HİI regions of our Galaxy, covers an angular extension of $\sim 36^\circ$ and is centered at $l^\circ = 258$, $b^\circ = -5$. Sahu (1992) analyzed the interstellar medium in the zone up to 2 kpc in Vela-Puppis; cometary globules and the star formation process in the Gum nebula have also been studied by Kim et al. (2005). Definitely, ζ Pup (O4If) and γ^2 Vel (WC8 + O7.5 I), the OB associations, Trumpler 10 and Vela OB2, seem to be the responsible entities of most of the photo-ionization in the nebula itself. To be remarked is the presence of the IRAS Vela Shell (Sahu, 1992), an expanding dust shell surrounding Vela OB2 with 6–8 pc radius enclosing the Gum nebula. Behind it, the Vela Molecular Ridge (Murphy and May, 1991), a superposition of giant CO molecular clouds, appears obscuring the farthest part of the Galaxy.

The purpose of the present investigation is twofold: on a side we want to re-discuss the parameters of five clusters in the TGQ onto the basis of a new set of photometry (one of them has never before been subject of *UBVI* photometry). On the other side, we want to connect the properties of these objects with the structure of Puppis and Vela associations and look for evidences of the grand design spiral structure. The photometric observations have been complemented with spectroscopy of several stars located in the cluster regions to discard field interlopers but also to estimate the absorption law. Table 1 lists coordinates of the clusters together with their angular sizes (from our analysis, in advance).

The remaining of the paper is organized as follows. In Section 2 we present and discuss the data acquisition of photometry and spectroscopy for five open clusters projected against the Vela Gum nebula. In Section 3 we illustrate the procedure applied for

Table 1
Cluster's radii from Section 3.1.

Cluster	α_{2000}	δ_{2000}	l°	b°	Radius [′]
Ruprecht 20	07 26 43	−28 49 00	242.451	−5.752	–
Ruprecht 47	08 02 19	−31 04 00	248.252	−0.188	4
Ruprecht 60	08 24 27	−47 13 00	264.106	−5.509	4
NGC 2660	08 42 38	−47 12 00	265.929	−3.013	6
NGC 2910	09 30 30	−52 55 06	275.310	−1.176	6

the derivation of fundamental parameters for the cluster sample. Section 4 presents a cluster-by-cluster discussion and the trend color excess. Discussion of the derived Galactic structure and our conclusions are given in Sections 5 and 6, respectively.

2. Observations and data reduction

2.1. Photometric data

We show in Fig. 1 the surveyed areas with CCD *UBV*(*I*) photometry of the five clusters in our sample enclosed by squares $\sim 4'$ on a side. NGC 2660 and NGC 2910 were measured at Las Campanas Observatory, Chile, on February 1996 with the 0.6-m telescope of the University of Toronto Southern Observatory (UTSO) equipped with a CCD PM 512 × 512 METHACROME-II UV coated camera. In these two clusters we carried out *UBVI* photometry. The scale of the CCD camera is $0.45''/pix$ what generates a field of $4'$ on a side. The nights were photometric with seeing values between $1.2''$ and $1.4''$. Four frames were necessary in the case of NGC 2910 to get the best possible coverage of the cluster.

CCD *UBV* photometry in Ruprecht 20, Ruprecht 47 and CCD *UBVI* observations in Ruprecht 60 were carried out at the CASLEO Observatory (Argentina) using the 2.15-m telescope equipped with a CCD ROPER 1300B, 1340 × 1300 pixels and $0.226''/pix$, covering $4.2'$ on a side. Ruprecht 47 was observed on the night March 9 (2005), Ruprecht 60 on April 3 (2005) and Ruprecht 20 on January 3 (2006). The typical seeing values for these observing runs varied from $1.3''$ to $2.1''$.

Details of exposure times and number of observations per filter for the five regions observed can be found in Table 2. In all cases, very short exposures were necessary to avoid saturation of the brightest stars.

Instrumental magnitudes were obtained by adjusting the PSF using the DAOPHOT package (Stetson, 1987) included within IRAF. To carry the instrumental magnitudes to the standard *UBVI* system, the following fields of standard stars were used:

- Ruprecht 20, standard stars from the list of Landolt (1992) and stars observed by Vogt and Moffat (1972) as secondary standards.
- Ruprecht 47, standard stars from the list of Landolt (1992), using the 10 stars observed by Vogt and Moffat (1972) in this cluster as secondary calibrators.
- Ruprecht 60, standard stars from the list of Landolt (1992).
- NGC 2910 and NGC 2660, a set of over 30 stars observed in open clusters NGC 5606 (Vázquez et al., 1994) and Trumpler 18 (Vázquez and Feinstein, 1990) was used.

The transformation equations to the standard system were of the form:

$$u = U + u_1 + u_2 \times X + u_3 \times (U - B)$$
$$b = B + b_1 + b_2 \times X + b_3 \times (B - V)$$
$$v = V + v_1 + v_2 \times X + v_3 \times (B - V)$$
$$i = I + i_1 + i_2 \times X + i_3 \times (V - I)$$

where u_2, b_2, v_2 and i_2 are the extinction coefficients for the *UBVI* bands, X are the air masses for each exposure and u_1, b_1, v_1, i_1, u_3, b_3, v_3, and i_3 the fitted parameters. The extinction coefficients were taken from Grotues and Gocherman (1992) for observations at Las Campanas Observatory and from Giorgi et al. (2007) for the CASLEO observations. Final photometric tables are available at CDS.

Table 3 shows in self explanatory format differences in magnitude and color indices together with the standard deviation of the mean between photoelectric/photographic and CCD data from several authors and our own data, except for Ruprecht 60, in the sense our measures minus other authors. The number of stars used in each comparison is indicated. Inspecting the differences we find an excellent agreement of our photometry with photoelectric measures for Ruprecht 20 and Ruprecht 47. However, strong magnitude and color off-sets appear in the case of NGC 2660. In this respect we want to mention that Sandrelli et al. (1999) do not mention they compared their photometry of NGC 2660 with previous values except for V, B and U isolated bands in a few stars (Sandrelli et al. is the most extended photometric study to date). What we see in Fig. 3 in Sandrelli et al. (1999) is a strong scatter around mean values when they compare to Hartwick and Hesser (1973) data. We are confident with the procedures we routinely undertake in doing photometry so we believe that the strong off-sets are due to zero point problems in Sandrelli et al. (1999) photometry. As for NGC 2910 we find a large discrepancy with Becker (1960) data and also with CCD data from Ramsay and Pollaco (1992). In the case of Ruprecht 60 no comparison is available since this cluster has only one study (Bonatto and Bica, 2010) made with J, H, and K_s bands of the Two-Micron All-Sky Survey (2MASS).

2.2. Spectroscopic data and MK classification

Spectra for MK classification purposes were collected at the 2.15-m telescope of CASLEO (Argentina) during several observing runs. The purpose of obtaining spectra of field stars in clusters is supported by the need of getting useful additional information from them to estimate precisely the visual absorption in each direction. These stars were selected primarily because of their brightness and then for the degree of proximity to the cluster center. They were observed according to the following detail:

- Ruprecht 20, 12 stars during three observing runs in January 2006, February 2007 and 2008.
- Ruprecht 47, 8 stars during two observing runs in January 2010 and February 2011.
- NGC 2660, 15 stars throughout several observing runs between 2002 and 2006.
- NGC 2910, 6 stars during two observing runs between 12–15 March (2002) and 12–13 March (2004).

Fig. 2 shows the spectroscopic finding charts. Numbers in the charts give the star identification used in this article. All spectra were obtained with the REOSC Cassegrain spectrograph attached to the 2.15-m telescope and the Tek 1024 × 1024 detector using a 600 l/mm grating in the first order. Spectra have a wavelength coverage from 3900 Å to 5500 Å (the traditional MK spectral region for classification from CaII K to H lines), 2.5 Å"/pixel dispersion (1800 resolution) and were reduced using standard procedures with IRAF. Our strategy for reducing cosmic rays and improve the signal/noise ratio consists in taking, at least, two spectra for each star with exposure times between 20 and 40 min depending on the star magnitude and seeing conditions. For the classification purpose we used MK standard stars taken with the same configuration at CASLEO and the Digital Spectra Classification of R.O. Gray

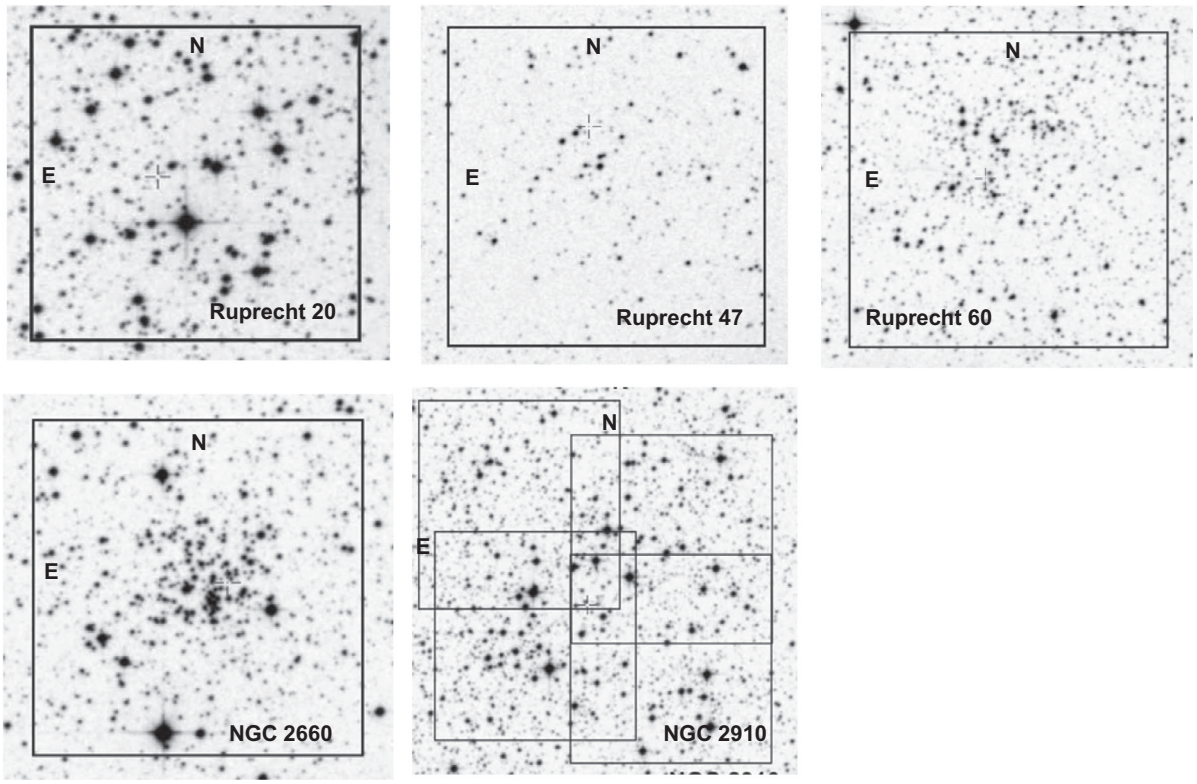

Fig. 1. Observed areas of the five clusters projected against *Digital Sky Survey* (DSS) images. Photometry has been performed within each black square $\sim 4'$ on a side. North and East are indicated.

Table 2
Exposure times for all clusters in seconds. In parenthesis is the number of averaged images.

Cluster	Exp time	Passbands			
		U	*B*	*V*	*I*
Ruprecht 20	*Medium*		3	3	–
	Long	300	300	300	–
Ruprecht 47	*Short*			10	2
	Medium		60	60	20
	Long	300	300	300	130
Ruprecht 60	*Medium*		30	30	20
	Long	300	300	300	130
NGC 2660	*Short*		200	100	2
	Medium				20
	Long	1000 (2)	1000	600	130
NGC 2910	*Short*	200	30	10	2
	Medium		200	100	20
	Long	1000 (2)	1000	600	130

"Digital Spectra Classification"[2] and "MK Standard Stars online" spectra.[3] An estimate by eye of the accuracy of our classification yields a potential half a sub-type as maximum departure from the right classification. Table 4 shows the MK spectral types obtained together with photometric magnitudes and color indices for all clusters but Ruprecht 60. Unfortunately, most of the brightest stars in the field of this cluster are too faint ($V \geqslant 13$ mag) to get an adequate compromise between the information obtained and a reasonable time consumption.

Finally we want to mention that for a number of stars discrepancies were found in the relative intensities of the K CaII lines and the spectral types assigned according to the H line intensities. This is, intensities of some Calcium lines belong to spectral types that are not exactly congruent with spectral types based in H lines. These peculiarities were found for stars in Ruprecht 20 and a description of them are given at the bottom of Table 4. Figs. 3–6 are the spectrograms of every stars we have classified in our clusters. Numbers in the figures are in our own notation indicated in Table 4.

[2] http://nedwww.ipac.caltech.edu/level5/Gray.
[3] http://stellar.phys.appstate.edu/Standards.

3. Getting the cluster fundamental parameters

In the following subsections we describe our method to analyze each cluster. Just to put the reader in the Galactic context we show in Fig. 7 the location of each of the five clusters in this study projected against a $\sim 40^\circ \times 40^\circ$ image of the Vela Gum adapted from the SHASSA SM-1 survey. Table 5 is a summary of fundamental parameters for all cluster as found in the literature (last raw in each cluster is the result from this work in advance).

3.1. Cluster sizes

Accuracy in cluster parameters is achieved only when star sequences sweeping a broad range of visual magnitudes are identified and when contamination for field interlopers is minimized. In this last aspect let us mention that cluster sizes are routinely used as criteria for separating cluster dominated from field-dominated regions in photometric diagrams (Vázquez et al., 2008). Although useful for recovering the precise locus occupied by cluster members, it is worth recalling that the cluster's linear size is a fundamental but overlooked quantity to characterize these objects. In fact, precise sizes are necessary for evaluating the cluster evolutionary status through analysis of its density and other related parameters (see Aarseth, 1996; de La Fuente Marcos,

Table 3
Differences with previous works in the sense this work minus other authors. N is the number of stars in common.

Cluster	Author	Data type	ΔV	$\Delta(B-V)$	$\Delta(U-B)$	N
Ruprecht 20	(1)	Photoelectric	0.01 ± 0.05	0.00 ± 0.03	0.01 ± 0.11	11
Ruprecht 47	(1)	Photoelectric	0.03 ± 0.04	0.04 ± 0.01	-0.03 ± 0.03	10
NGC 2660	(2)	CCD ($V < 16m$)	0.14 ± 0.04	-0.02 ± 0.04	-0.15 ± 0.08	163
		CCD ($V < 19m$)	0.14 ± 0.07	0.00 ± 0.10	-0.20 ± 0.10	381
NGC 2910	(3)	Photoelectric	0.00 ± 0.30	-0.20 ± 0.30	0.20 ± 0.60	39
	(4)	Photographic	0.00 ± 0.10	0.00 ± 0.10	0.20 ± 0.10	37
	(5)	CCD	-0.04 ± 0.09	0.1 ± 0.20	0.12 ± 0.07	58*

References: (1) Vogt and Moffat (1972); (2) Sandrelli et al. (1999); (3) Becker (1960); (4) Topaktas (1981); (5) Ramsay and Pollaco (1992).
* Ramsay and Pollacco (1994) give $(U-B)$ data for only 17 stars.

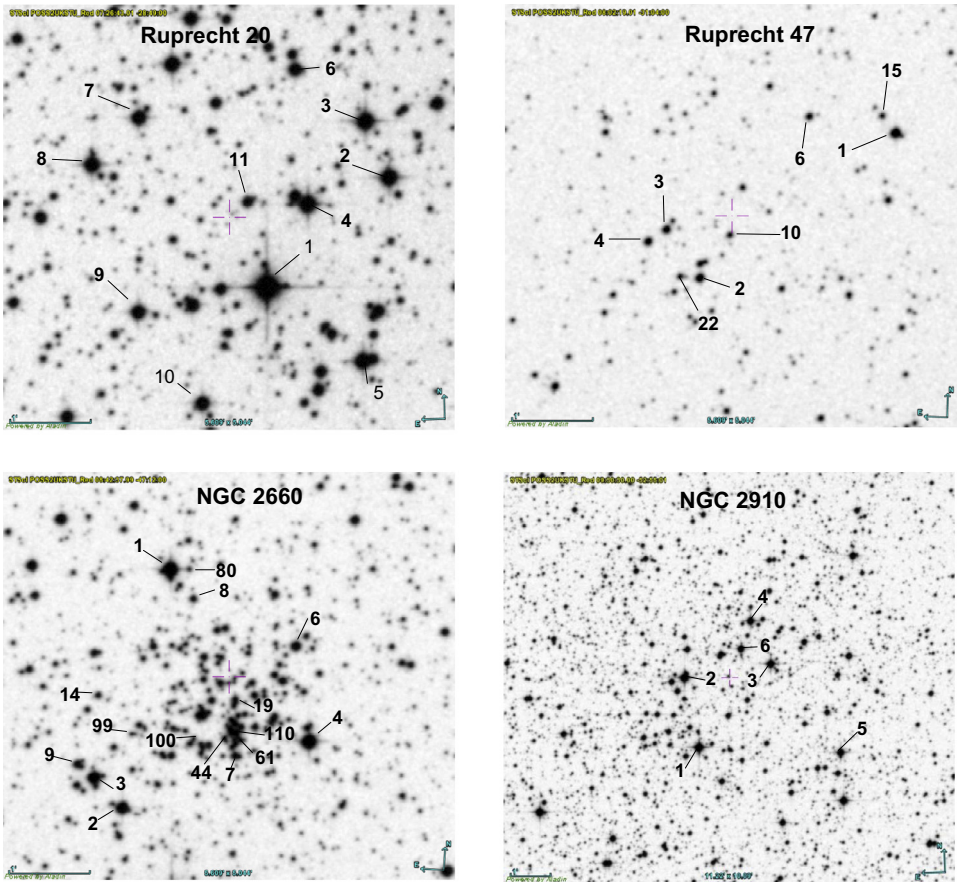

Fig. 2. Spectroscopic finding charts. Numbers are in the notation used in this work (see Table 4). North and East as in Fig. 1.

1997; Kroupa et al., 2001) such as the slope of the mass spectrum. Usually, cluster sizes are computed by assuming a centrally peaked spherical stellar distribution and then determining the distance at which its radial density profile merges with the (flat) density of the stellar background. In practice, this determination is normally done either by visually setting this limit in a density radial plot or analytically by fitting a King (1962) profile to an observed radial density profile. In both approaches a spherically symmetric distribution is assumed what may not be true since open clusters are, by definition, irregular in shape. Moreover, in the case of the King profiles, it is assumed that the system is dynamically relaxed too. Since a good size estimation reduces quite considerably the field star contamination, we restrict the analysis to stars within the cluster limits.

Our starting point consists in adopting cluster center coordinates given in available catalogs (e.g. WEBDA) and counting the number of stars found in concentric rings $0.5'$ in width around them. Instead of using our own photometry we use 2MASS[4] data (the three bands but particularly the deepest K band) that cover areas larger than ours. This way we ensure the reliability of the cluster sizes and overcome the effects from visual absorption. The star counts were divided by the area of each ring following well established receipts (e.g. Carraro et al., 2007). Fig. 8 shows density profiles for the 5 clusters in our sample. Vertical error bars in the density profiles are computed as the square root of the number of stars divided by the ring surfaces. The radius of each cluster (see Table 1) is shown by an arrows in the point where the cluster density merges with the field stellar density level approximately (solid lines in Fig. 8). In all the cases we estimated the field density level by eye.

Finally, comparing Figs. 1 and 8 we want to emphasize that since cluster radii are larger than the areas we have surveyed our

[4] http://www.ipac.caltech.edu/2mass/.

Table 4
MK spectral classification for stars in four of the five clusters.

Cluster	Old ID	Our ID	MK ST	V	$(B-V)$	$(U-B)$	E_{B-V}	M_V	$d_\odot$ [kpc]
Ruprecht 20	VM72 1	1	A5III	8.79	0.28	0.12	0.13	0.70	0.34
	VM72 2	4	K0III	11.60	1.03	0.78	0.03	0.70	1.45
	VM72 3	6	K7III	11.64	1,57	1.76	0.04	−0.30	2.28
	VM72 4	7	K7III	11.67	1.58	1.73	0.05	−0.30	2.05
	VM72 5	8	K7III	11.91	1.31	1.16	0.00	−0.30	2.77
	VM72 6	10*	B8V	12.65	0.16	0.14	0.27	−0.25	2.56
	VM72 7	2	A5IV	11,69	0.19	0.17	0.04	1.30	1.13
	VM72 8	5	F0III	12.11	0.42	0.20	0.12	1.50	1.10
	VM72 9	3	B9V	12.04	0.04	−0.07	0.11	0.20	1.99
	VM72 10	9*	F8III	12.39	0.56	0.10	0.00	1.30	1.60
	VM72 11	18*	F8V	13.81	0.49	0.062	0.00	4.00	0.95
		16	G2V	13.48	0.64	0.22	0.01	4.70	0.56
Ruprecht 47	VM72 1	4	A0V	12.01	0.22	0.10	0.24	0.65	1.33
	VM72 2	3	A1V	11.92	0.26	0.13	0.27	1.00	1.04
	VM72 3	2	B5Ve	11.52	0.17	−0.46	0.34	−1.20	2.16
		22	G1.5 V	13.70	1.11	0.68	0.51	4.60	0.32
	VM72 4	10	B1V	12.98	0.16	−0.38	0.42	−3.20	9.46
	VM72 7	6	B7V	12.50	0.15	−0.36	0.28	−0.60	2.79
		15	F2V	13.41	0.50	0.08	0.15	3.60	0.74
	VM72 8	1	F0V	10.93	0.43	0.13	0.13	2.70	0.40
NGC 2910		1	B7III	9.69	0.03	−0.43	0.15	−1.50	1.40
		2	B7III	9.97	0.10	−0.24	0.22	−1.50	1.44
		3	F8V	10.70	0.51	0.07	0.00	4.00	0.22
		4	B5Vp	10.77	0.08	−0.34	0.24	−1.20	1.76
		5	B8III	10.80	0.15	−0.11	0.27	−1.20	1.71
		6	B8V	11.05	0.06	−0.18	0.17	−0.25	1.43
NGC 2660		1	K0II	10.75	1.26	0.98	0.18	−2.30	3.15
		2	K0III	12.17	1.38	1.33	0.38	0.70	1.14
		3	K0III	12.18	1.72	1.56	0.72	0.70	0.71
		6	K0III	13.17	1.27	0.95	0.27	0.70	2.12
		7	A1V	13.91	0.47	0.39	0.49	0.65	2.23
		8	B8III	13.91	0.32	−0.16	0.43	−1.20	5.69
		9	F8III	13.97	1.05	0.57	0.51	1.20	1.73
		14	F0V	14.36	0.53	0.32	0.21	2.70	1.59
		19	F8V	14.40	1.26	0.93	0.33	4.00	0.75
		44	F2Vp	14.85	0.68	0.28	0.33	3.00	1.46
		61	F8IIIp	15.13	0.88	0.40	0.34	1.20	3.76
		80	F6Vp	15.32	0.71	0.39	0.27	3.50	1.57
		99	F2Vp	15.68	0.60	0.33	0.25	3.00	2.40
		100	F6Vp	15.68	0.65	0.27	0.21	3.50	2.02
		110	F8Vp	15.80	0.70	0.28	0.18	4.00	1.77

ln Old ID column VM72 refers to Vogt and Moffat (1972) numbering.
Ruprecht 20 *: 10 KCaII(A1V), H(B8V) (broadened lines); 9 KCaII(F0), H(F8III); 18 KCaII(F8), H(F8), GB(F8), Mgab(F0).

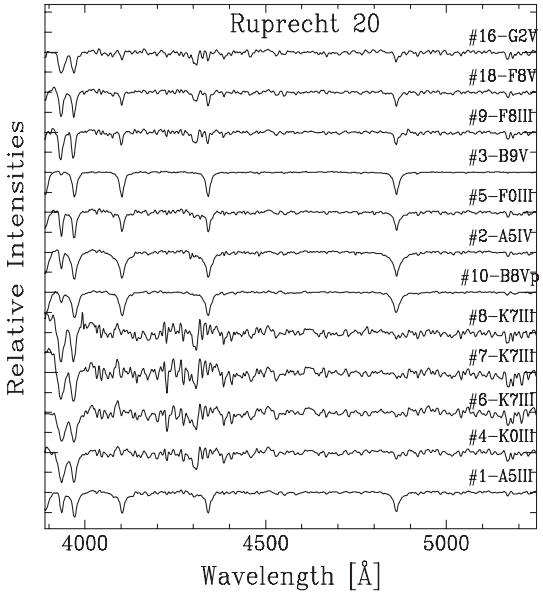

Fig. 3. Spectra of stars in Ruprecht 20. Numbers indicate stars identified in Table 4.

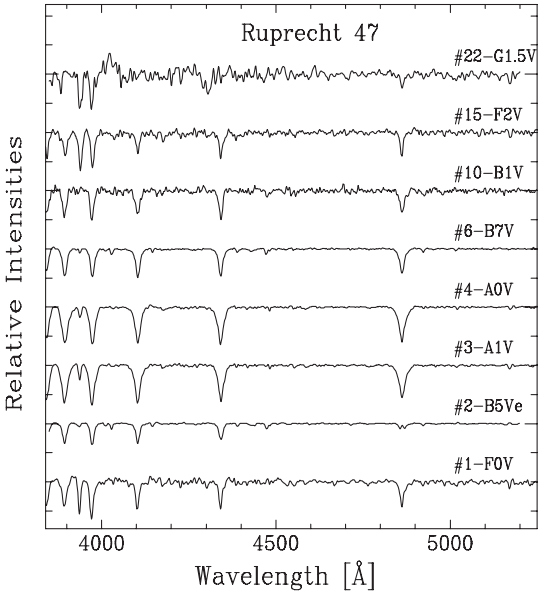

Fig. 4. Idem Fig. 3 for stars in Ruprecht 47.

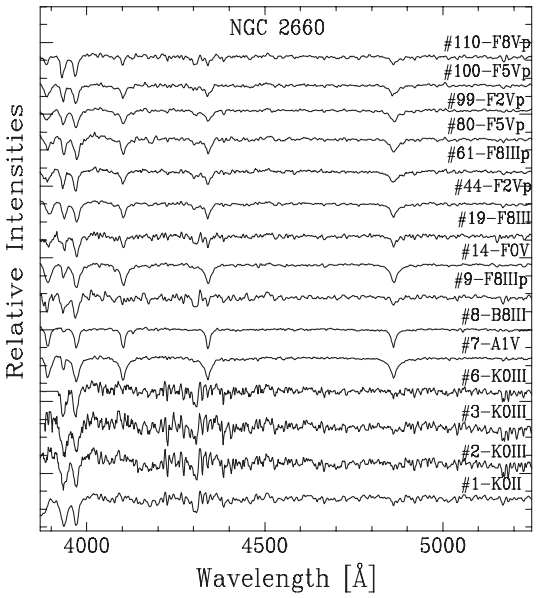

Fig. 5. Idem Fig. 3 for stars in NGC 2660.

observations are entirely contained within the cluster boundaries and therefore we do not expect high contamination by field interlopers. Thus, we are confident that our observations are useful to yield realistic cluster parameters.

3.2. Memberships

Open clusters are usually not far from the Galactic plane and appear therefore projected against crowded stellar fields and immersed in regions of high absorption. This makes the membership assignment a difficult task, particularly amongst faint stars. All across this article we address memberships applying the classical method of checking simultaneously the consistency of the location of each star in several photometric diagrams (two color diagrams, hereinafter TCDs, and different color-magnitude diagrams, hereinafter CMDs). This method is an efficient tool when membership estimates rely on a careful inspection of the TCD and consistent reddening solutions are applied. Contamination for field interlopers is dramatic in crowded fields and may lead, on a side, to bad membership assignments and, on the other consequently, to wrong cluster parameters. It happens the turn-off point position may be strongly affected by interlopers even in the bright portion of the CMDs. However, we use the $(U-B)$ index that is much more sensitive to stellar temperature changes than the $(B-V)$ index (Meynet et al., 1993) so that the V vs $(U-B)$ CMD is quite useful for eliminating most of A-F-type field stars contaminating precisely the vertical part of the cluster sequences, especially of young clusters.

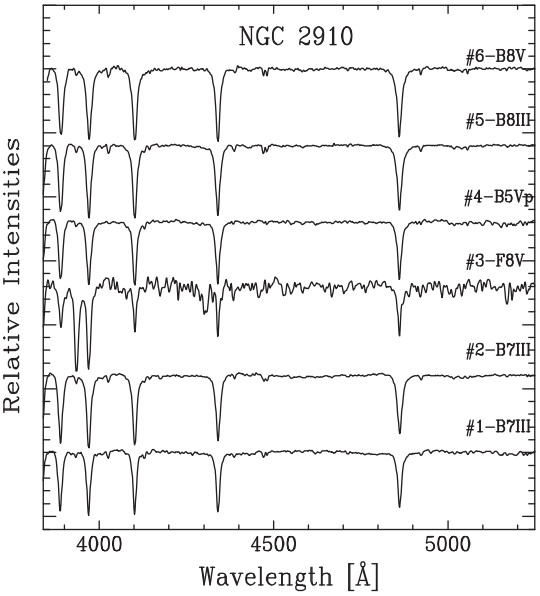

Fig. 6. Idem Fig. 3 for stars in NGC 2910

3.3. Reddening, distances and ages

The reddening value $E_{(B-V)}$ in each cluster has been computed by superposition of the Schmidt-Kaler (1982) [SK82 hereinafter] ZAMS in the TCD of the cluster. We shift the ZAMS along the reddening line (given by the standard relation $E_{(U-B)} = 0.72 \times E_{(B-V)} + 0.05 \times E^2_{(B-V)}$) until the best fit to the cluster sequence is achieved. On the other hand, the knowledge of the ratio of total to selective absorption, $R \times E_{(B-V)} = A_V$, must be well established to compute a confident cluster distance. Though the analysis in Moitinho (2001) carried out for several open clusters in the TGQ suggests that the extinction law is normal, an additional check of the R–value was performed in the $(B-V)$ *vs* $(V-I)$ plane in Ruprecht 60, NGC 2660 and NGC 2910. In this diagram, if the slope of the standard reddening line $E_{(V-I)}/E_{(B-V)} = 1.244$ (Dean et al., 1978) follows the stellar distribution this fact means the extinction law is $R = 3.1$. Apparent cluster distance moduli were derived then by superposing the SK82 ZAMS onto the observed cluster sequences and the cluster distances from the Sun ($d_\odot$) are obtained after removing absorption from apparent moduli. The fitting error in each cluster was estimated by eye inspection.

As for cluster ages they were derived under the assumption clusters are of solar metal content. We superposed isochrones produced by Girardi et al. (2000) onto the cluster sequences (once they have been well established) putting special emphasis in fitting not

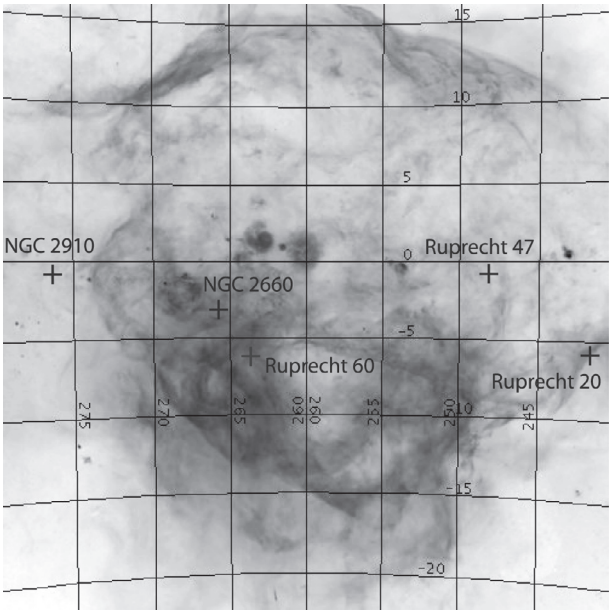

Fig. 7. The five clusters (plus symbols) in the present sample projected against an Hα full sky map image toward the Vela Gum nebula directions. Grid is in Galactic coordinates.

Table 5
Earlier and present study results in the five clusters.

Clusters parameters					
Cluster	α_{2000} δ_{2000}	Source	$E_{(B-V)}$	$d_{\odot}$(kpc)	Age (Gyr)
Ruprecht 20	$7^h26^m43^s - 28°49'$				
		Vogt and Moffat (1972)	0.1	1.21	–
		This work	–	–	–
Ruprecht 47	$8^h02^m19^s - 31°04'$				
		Vogt and Moffat (1972)	0.28	3.03	–
		Kharchenko et al. (2005)	0.25	3.01	0.11
		This work	0.32 ± 0.02	4.1 ± 0.4	0.06–0.08
Ruprecht 60	$8^h24^m27^s - 47°13'$				
		Bonatto and Bica (2010)	0.64 ± 0.1	6.16 ± 0.88	0.4 ± 0.1
		This work	0.37 ± 0.05	4.2 ± 0.2	0.8–1.0
NGC 2660	$8^h42^m39^s - 47°12'$				
		Hartwick and Hesser (1973)	0.38 ± 0.05	2.88 ± 0.01	1.20
		Lyngä (1987)	0.35	2.1	1.58
		Hesser and Smith (1987)	0.35 ± 0.03	4.35	–
		Frandsen et al. (1989)	0.36	2.9	1.2
		Geisler et al. (1992)	0.37 ± 0.05	–	1.7
		Friel (1995)	–	2.89	0.8
		Sandrelli et al. (1999)	0.37–0.42	2.63–2.88	< 1
		This work	0.33	2.7 ± 0.2	~ 1.58
NGC 2910	$9^h30^m22^s - 52°54'$				
		Becker (1960)	0.09	1.25	0.04
		Topaktas (1981)	0.05	1.32	–
		Ramsay and Pollaco (1992)	0.11 ± 0.02	1.45 ± 0.01	< 0.3
		Kharchenko et al. (2005)	0.34	2.61	0.03
		This work	0.22 ± 0.05	1.3 ± 0.1	0.06

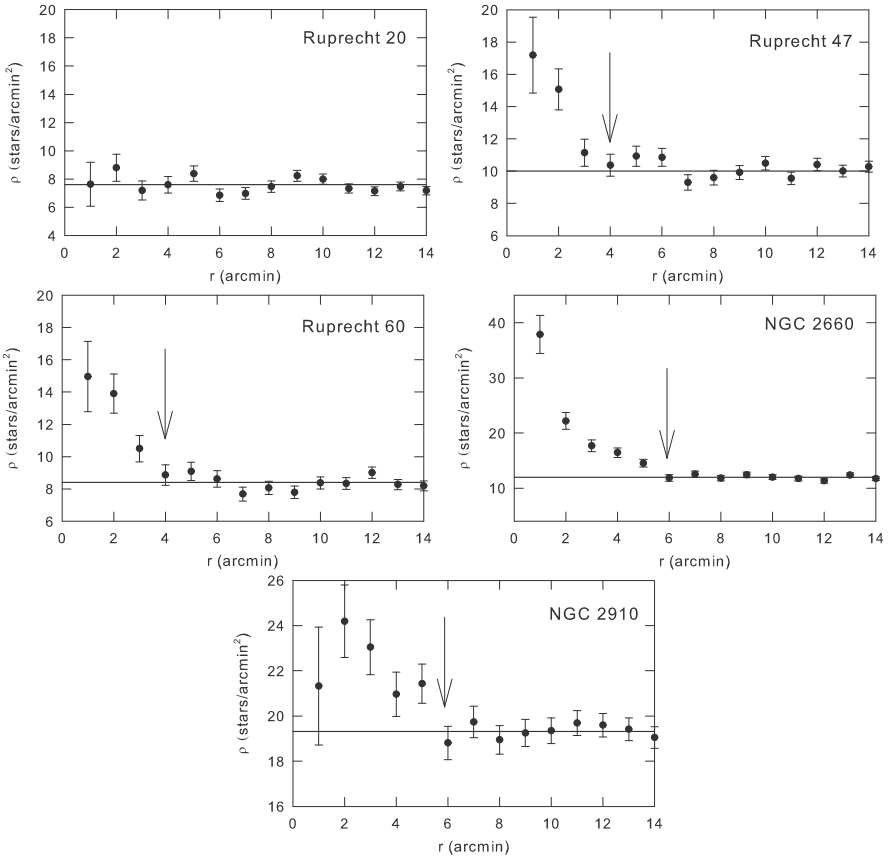

Fig. 8. Radial density profiles derived in the five clusters with 2MASS data. The arrows indicate the point at which the radial density merges with the background star density **shown by solid lines**.

only probable members in the upper sequence but also covering the largest possible magnitude range. However, in four out of the five clusters we were forced to use two ischrones to establish an age range. Various factors such as remaining material from the star formation processes (affecting young clusters), undetected binary stars or unresolved double stars, altogether scatter stars around the mean sequence causing difficulties to achieve a good fit by a single isochrone. In older clusters these difficulties are amplified because of the need to fit simultaneously main sequence and red clump stars as we show in Sections 4.3 and 4.4.

3.4. Reddening and distances of stars with spectral types

Spectral types are a powerful and independent tool to estimate distances and color excesses of individual stars and become indispensable to corroborate distances to open clusters. Combining MK types and *UBV* photometry we can easily get the distance of individual stars via the well know spectroscopic parallax method. In the cases of stars in Table 4 we proceed to assign intrinsic $(B-V)_0$ and $(U-B)_0$ colors based in MK types following the relations given in SK82. Intrinsic colors according to MK types and observed colors allow to get the reddening $E_{(B-V)}$ and derive the A_V to produce free absorption magnitudes V_0 mag using the expression given below. In a couple of late type stars the reddening turned out to be negative. We think this is due to the low reddening of these stars and uncertainties in the true colors of evolved stars. In these cases we adopt a reddening value $E_{(B-V)} = 0.0$. Combining the MK types with absolute magnitudes M_V using SK82 relations we are able to get individual star distances. The main sources of errors in distances come from photometric uncertainties in color and magnitudes. This is, the formula:

$$V - M_V = -5 + 5\log d + A_V \quad (1)$$

leads to an error in distance $\epsilon(d)$ of the form:

$$\epsilon(d) = \ln 10 \times d \times 0.2[\sigma_V + 3.1\sigma_{B-V}] \quad (2)$$

where σ_V and σ_{B-V} are typical photometric errors in our sample.

This procedure has been successfully applied in Perren et al. (2012). In the current case, we assume no error in the extinction law ($R = 3.1$) and no error in the absolute magnitudes (M_V) of the stars. The photometric errors of individual stars with spectral types are all below 0.04 which means that errors in distances derived with the spectroscopic parallax method are all below 10%. Table 4, columns 8–10, contains the estimated $E_{(B-V)}$ excesses, adopted M_V and distances for isolated stars with spectral types.

4. Cluster by cluster analysis

4.1. Ruprecht 20

Ruprecht 20 was studied by Vogt and Moffat (1972) who obtained *UBV* photoelectric photometry for 11 stars. Although their work calls into question the existence of a true cluster in this region, they assume that stars number 10, 3 and 18 (our ID) [6, 9 and 11 in Vogt & Moffat notation] are potential members of luminosity class V (their assumed luminosity classes are confirmed by our spectroscopy in Table 4 but we do not agree they are potential members of Ruprecht 20). Vogt and Moffat (1972) obtained the following cluster parameters $E_{(B-V)} = 0.1$, $V - M_V = 11.04$ and $d_\odot = 1.21$ kpc in case it is a real entity. This cluster has been subject also of a specific survey aimed at determining radial velocity amongst red giants to secure memberships (Mermilliod et al., 2008). These authors could find two red giant stars that they assumed likely cluster members.

According to our data the cluster radial density profile of Ruprecht 20 shown in Fig. 8, upper left panel, does not suggest the presence of an open cluster since no star grouping is evident. Indeed, the density profile resembles the typical profile produced by random stellar fluctuations.

Fig. 9 includes from left to right the V *vs* $(B-V)$, $(U-B)$ *vs* $(B-V)$ and the V *vs* $(U-B)$ diagrams. In the TCD, middle panel, we superpose the ZAMS shifted by $E_{(B-V)} = 0.1$ according to Vogt and Moffat (1972) and, simultaneously, we show the ZAMS fitted to the apparent distance modulus $V - M_V = 10.73$ ($d_\odot = 1.21$ kpc) suggested by them too. It is simple to see that no cluster sequence is accompanied by this ZAMS fitting or, in other words, it is hard to perceive a cluster sequence in these diagrams. Instead, we see a sparse handful of stars, some of them affected by a similar amount of reddening, $E_{(B-V)} = 0.1$, but no traces of any cluster. This is, exactly, what Fig. 8 indicates.

We find the respective distances for the 10 stars with MK spectral types (see Table 4). According to their classifications, stars 10, 3 and 18 (our ID) are located at distances of approximately 2.55, 1.99 and 0.95 kpc respectively, demonstrating beyond any doubt they do not belong to any stellar aggregate. The distance of stars 10

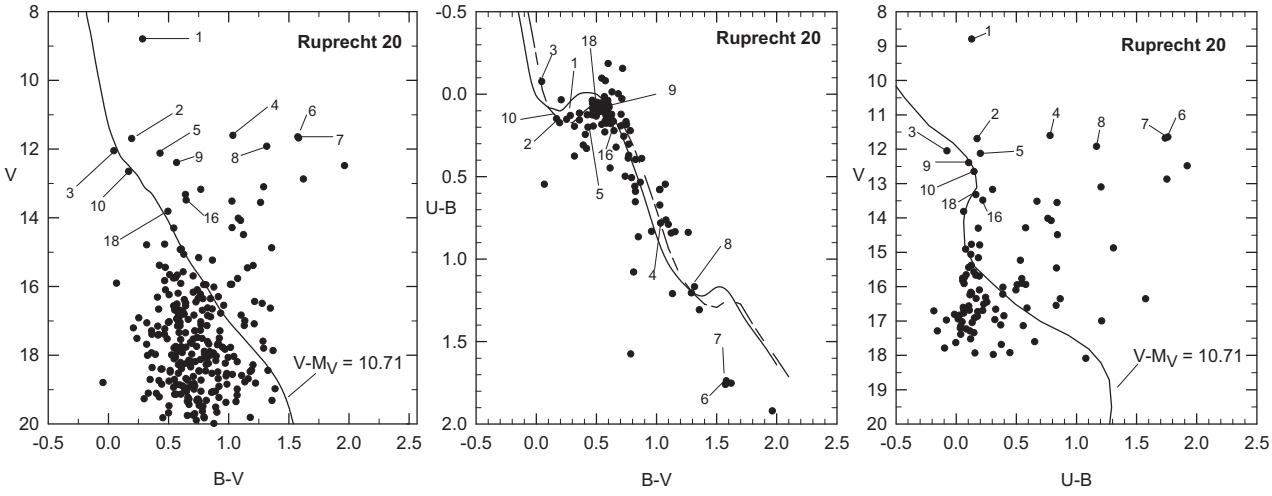

Fig. 9. From left to right: V *vs* $(B-V)$ CMD, $(U-B)$ *vs* $(B-V)$ TCD and V *vs* $(U-B)$ CMD for Ruprecht 20. Stars with MK types are pointed out. The SK82 ZAMS (dashed line) has been fitted to an excess value $E_{(B-V)} = 0.1$ in the TCD. Solid lines in the CMDs are the SK82 ZAMS fitted to an apparent distance modulus $V - M_V = 10.71$ as suggested by Vogt and Moffat (1972). See text for details.

and 3 are of the order of the distance of star 6 (~ 2.30 kpc). But this last is of late evolved type, a K7III, while star 6 is a B8V and star 9 is a B9V.

In short, the CMDs and the TCD of Ruprecht 20 confirm that no cluster exists in this location but we are dealing with a sparse group of stars mostly of dwarf and giant-types. To mention is the fact that above the second knee of the ZAMS there are some stars that are hard to interpret. They are located along the path of the reddening in the TCD and could be very reddened blue stars. However, they are too faint. They could be sdB type stars but since their average absolute magnitudes are $\sim +5$ and our magnitude cut-off is $V = 17$ mag we do not expect more than a tenths of sdB stars in our frames. Certainly, spectroscopy could help to solve the nature of these objects.

After the above analysis we understand that evidences provided by our photometry and spectral analysis are irrefutable and we conclude that the open cluster Ruprecht 20 is not a physical entity. In our opinion the connection of two red giant stars as suggested by Mermilliod et al. (2008) with this object is unrealistic.

4.2. Ruprecht 47

Ruprecht 47 also was studied by Vogt and Moffat (1972), who carried out photoelectric photometry on 10 stars. Through these observations they placed the cluster at a distance from the Sun of 3.03 kpc but, since their observations were limited to only a few stars on the upper main sequence, the authors suggest the true distance value can be quite different. Kharchenko et al. (2005) also studied this cluster and found 7 probable members at a distance of the order of 3 kpc with a reddening similar to the obtained by Vogt and Moffat (1972).

This case is quite different from the one of Ruprecht 20. In principle, the radial density profile in Fig. 8 upper right panel shows a clean star density profile extending up to 4′ where it merges with the background star density. This fact suggests we are in the presence of a star overdensity.

Fig. 10, the CMDs and TCD, show in turn a well defined star sequence proper of a relatively young open cluster because of the presence of several blue stars in the TCD (middle panel). Numbers (our notation) in the diagrams point out stars with spectral types. The superposition of the ZAMS in the TCD yields average color excesses of $E_{(B-V)} = 0.32 \pm 0.03$ and $E_{(U-B)} = 0.23 \pm 0.04$, a bit larger than earlier studies in Table 5 but still, within 3σ, in agreement with Vogt and Moffat (1972) though quite far from the value found by Kharchenko et al. (2005). In our interpretation, our reddening value is more robust than previous ones since we can cover the cluster sequence till the second knee in the TCD, the scatter of the data is low in this diagram and the mean differences with Vogt and Moffat (1972) data are all quite acceptable.

The fitting of the SK82 ZAMS to the main sequence in the V vs $(B-V)$ and V vs $(U-B)$ diagrams yielded an absorption free distance modulus of $V_0 - M_V = 13.2 \pm 0.2$, corresponding to a distance of $d_\odot = 4.4 \pm 0.4$ kpc. This result is quite different from earlier values determined by Vogt and Moffat (1972) and

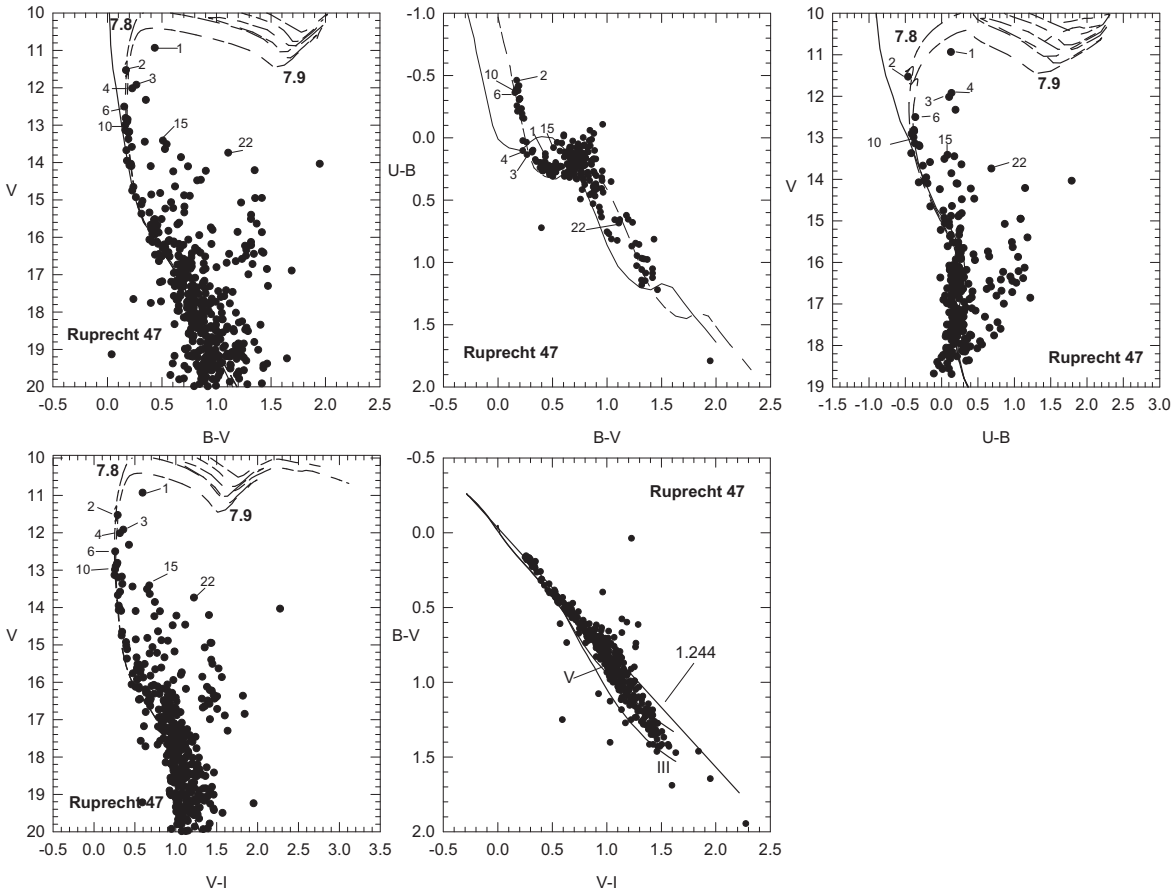

Fig. 10. Upper panels from left to right: V *vs* $(B-V)$ CMD, $(U-B)$ *vs* $(B-V)$ TCD and V *vs* $(U-B)$ CMD. Solid line in the TCD is the SK82 ZAMS in its normal position while solid lines in the CMDs are the SK82 ZAMS fitted to the cluster distance modulus. Dashed line in the TCD is the ZAMS shifted by a reddening $E_{(B-V)} = 0.32$. The respective isochrone matchings in the CMDs are indicated by dashed lines. Bold numbers by the isochrones are the $\log(t)$. Left lower panel is the V *vs* $(V-I)$ CMD. Lines as in the upper panels. Right lower panel is the color–color $(B-V)$ *vs* $(V-I)$ diagram including the intrinsic relations for stars of luminosity classes V and III from Cousins (1978). The line with slope 1.244 is the path of the reddening in this last plane and agrees with $R = 3.1$. Stars with MK spectral types are all pointed out, see text for details.

Kharchenko et al. (2005) for more that 1 kpc. So far as we can interpret the data the explanation for such a difference must be found in a simple fact already mentioned: our definition of the cluster in the TCD is very good and, in addition, we can track the cluster main sequence down to $V = 16$ mag in the CMDs. This means a larger range of apparent magnitudes that allows to achieve a better ZAMS superimposition and therefore more precision in the cluster distance.

The cluster age was derived by matching the Girardi et al. (2000) isochrones (dashed lines in the CMDs in Fig. 10). The best possible matches were achieved for ages between 63 and 80 million years ($7.8 \leqslant \log(t) \leqslant 7.9$). There is, as expected from the difference in distance between this work and earlier ones, a significant difference between our age value and the 117 million years from Kharchenko et al. (2005). We think that the age difference found is closely related with our ability to locate precisely the cluster "turn-off" point at $V \sim 1.5$ mag. In fact, that is why we differ from Kharchenko et al. (2005) who derived the cluster parameters taking into account stars down to $V \approx 13$ mag. Certainly, since they had no opportunity to see this point their distance and age were weakly determined.

Spectral types in the region of Ruprecht 47 include 8 bright stars listed in Table 4 and pointed out in the corresponding panel of Fig. 10. Three of them are of B-type, one, number 2 in our notation, is an emission B5Ve star. Because of the small β-value, Vogt and Moffat (1972) suggested it is an emission object that we confirm with our spectroscopy. Inspecting distances shown in Table 4 we conclude that none of these 8 stars with spectroscopic parallaxes have chances to become cluster members since they are, on the average, twice closer to the Sun than the cluster Ruprecht 47 situated at (≈4 kpc). This negative result is very interesting since without a spectroscopic analysis most of the bright stars in this cluster would have been assumed cluster members. The astrophysical impact of such an error is clear; it produces an over-estimation of the number of massive stars in the cluster head and severely modifies the cluster initial mass function value (out of the scope of the our investigation). That is why spectroscopy is so valuable. Now, it is obvious the presence of other blue stars in the TCD of Ruprecht 47 and one may wonder how much field interlopers modify the cluster parameter. We do not know the answer but we have been as careful as possible in isolating the cluster region using star counts. This said, we shall assume as likely cluster members the other blue stars in Ruprecht 47 until the contrary is demonstrated. Another interesting result from the of spectroscopic parallaxes has to do with star 10 (in our notation). This is a very early-type star, B1V, affected by an amount of reddening comparable to the rest of stars. But quite surprisingly, this object is a remote star located at almost 9.5 kpc from the Sun. If our distance estimate is not wrong, this star becomes a serious candidate to be member of the innermost part of the Outer Arm. We discuss in Section 5 the interpretation of this star in the framework of the nearby Galaxy structure.

4.3. Ruprecht 60

Ruprecht 60 has been studied by Bonatto and Bica (2010) through 2MASS photometry using a decontamination algorithm developed by them. These authors stated the cluster is affected by a reddening over $E_{(B-V)} = 0.6$ and placed it at a distance of more than 6 kpc. The age they found for Ruprecht 60 is 4×10^8 yr.

This is the first time that *UBVI* photometry is undertaken in this overlooked object, probably, due to its weakness. In fact, images from the *Digital Sky Survey* (DSS) show an almost irrelevant group of faint stars concentrated in a small portion of the sky as seen in Fig. 1 (left middle panel). Notwithstanding, our photometry that reaches stars as faint as $V \sim 21$ mag is quite concluding since the radial density profile shown in the middle left panel in Fig. 8 confirms it is a true open cluster. On the other hand, the extreme weakness of the brightest stars in this object (they have magnitudes of $V \approx 14.5$) precluded us from taking spectra in a reasonable amount of observing time. So, our analysis of this cluster rests upon photometric data alone.

Fig. 11 shows the CMDs V *vs* $(B-V)$, upper left panel, and the V *vs* $U-B$, upper right panel, of Ruprecht 60. The middle upper panel represents the corresponding TCD. In the lower left panel we show the V *vs* $V-I$ CMD and in the lower right panel the $(B-V)$ *vs* $(V-I)$ color–color diagram. The $(U-B)$ *vs* $(B-V)$ TCD shows very few stars with $U-B$ inside the cluster area and therefore with the highest chances to be physically related to the cluster. We can fit these stars by shifting the intrinsic line by $E_{(B-V)} = 0.37 \pm 0.05$ and $E_{(U-B)} = 0.27 \pm 0.05$. These values are, in our interpretation of the TCD, the most probable color excesses of Ruprecht 60. This is, we interpret there is no way the color excess of this cluster is $E_{(B-V)} = 0.64 \pm 0.1$ as claimed by Bonatto and Bica (2010). More interesting is the V *vs* $(B-V)$ CMD where a tight cluster main sequence dominates in the range $15 \text{ mag} < V < 19 \text{ mag}$. A worse isolation of this sequence is achieved in the V *vs* $(V-I)$ CMD since the scatter of $(V-I)$ data is much more pronounced. In all the CMDs, the V *vs* $(B-V)$ and V *vs* $(V-I)$ particularly, the cluster sequence shows evidences of evolution as stars leave the main sequence at $V \sim 16.5$ mag.

Since the color excess of the cluster turned out to be $E_{(B-V)} = 0.37$ we compute the cluster distance by adjusting the SK82 ZAMS in the CMDs V *vs* $(B-V)$ and V *vs* $(U-B)$ achieving the best fit for an apparent distance modulus of $V - M_V = 14.25 \pm 0.10$. This corresponds to a true distance modulus of $V_0 - M_V = 13.1$ that places Ruprecht 60 at a distance of $d_\odot = 4.2 \pm 0.2$ kpc. The absorption law, that we use to get the absorption-free parameter above is $R = 3.1$ as evidenced by Fig. 11, lower right panel.

A precise estimation of the age of clusters with some degree of evolution, as this is the case, is certainly complex in terms of the morphology of the turn-off point. In fact, as summarized in Friel (1995), the number of binary stars and blue stragglers in the field of old open clusters has important implications in interpreting the color-magnitude diagram and their comparison with theoretical models, since the morphology of the turn-off region is strongly affected by the presence of composite systems. When binary systems evolve through the turn-off region of single/simple stars, a color enlargement of the CMD diagram occurs near this point and the systems move toward larger luminosity than that of the true turn-off, before evolving into the region of red giants. Apart from this, many old open clusters show stars in the blue straggler region of the color-magnitude diagram, above and to the blue of the main sequence turnoff. Radial velocity studies indicate that a significant number of stars found in this region are members of clusters and, among them, the spectroscopic binary frequency exceeds 40% (Milone, 1992; Friel, 1995). The intersection of the evolutionary paths of single stars and binary systems creates thus a more complex color and luminosity distribution precisely in the region near the turn-off, where clarity is necessary in order to adjust the set of isochrones and determine the age based on the position of this point. In Ruprecht 60 CMDs we do not see a potentially large number of candidates to blue straggler if any. As for the presence of binary systems there is nothing we can say since our observations were not designed for detecting this type of objects. Therefore, and under the hypothesis that this cluster is solar metal content, the best fit for the set of isochrones by Girardi et al. (2000) yielded, after several tries, an age range between 800 and 1000 million years ($8.9 \leqslant \log(t) \leqslant 9$) as shown in Fig. 11.

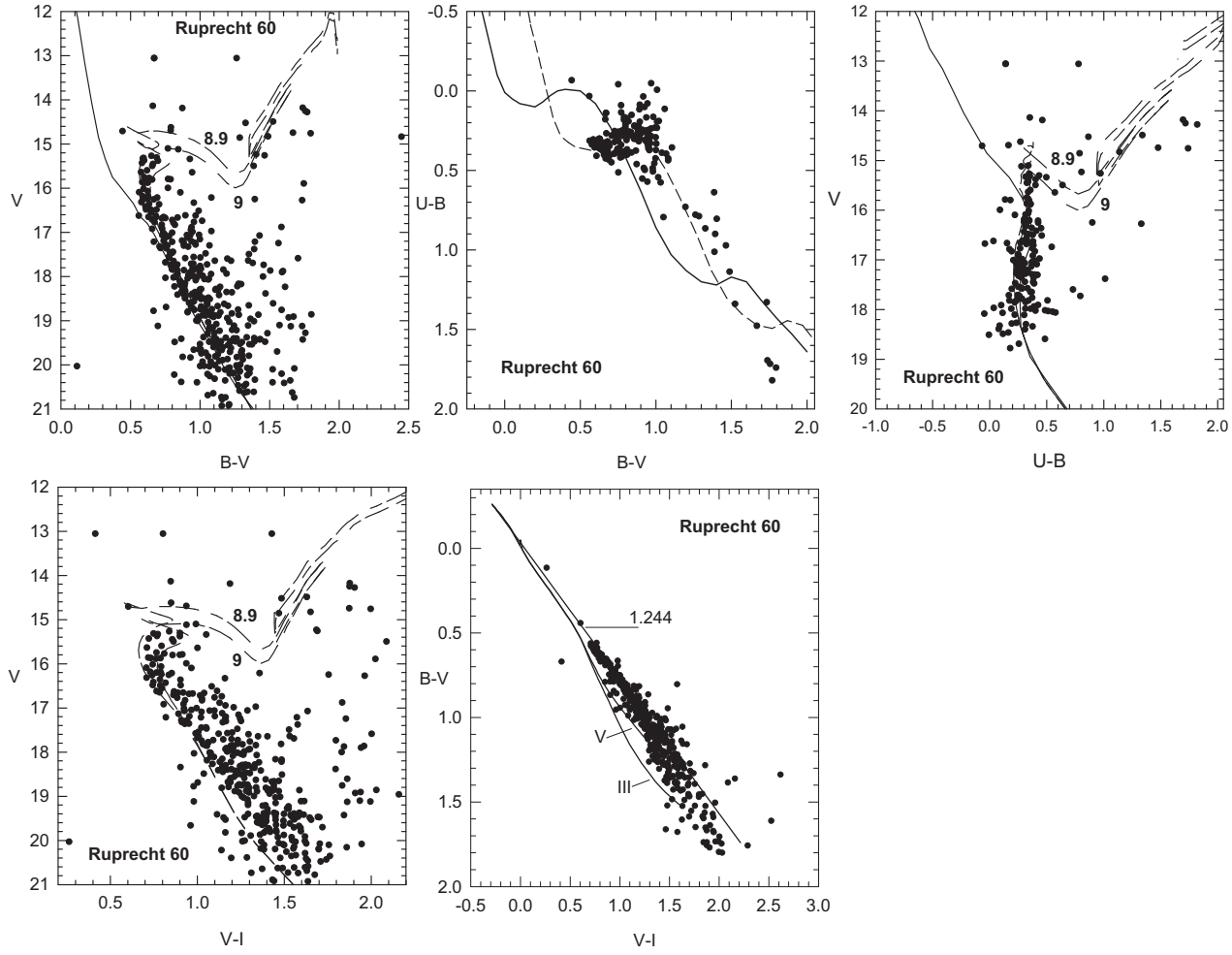

Fig. 11. Upper and lower panels as in Fig. 10. Idem for symbols and lines. The ZAMS in the TCD is shifted by a reddening $E_{(B-V)} = 0.37$.

Our data analysis yielded results quite different from Bonatto and Bica (2010). In fact, they have found, as seen in Table 5, a larger reddening and a larger distance (almost 50%) than ours. And, in terms of the cluster age, ours is larger by a factor of more than 2. Even though these authors applied a less personal method (more sophisticated too) to estimate cluster parameters, we interpret that these differences (cluster size aside) come from the use of *JHK* 2MASS photometry. That is, getting the cluster reddening using *IR* photometry may lead to wrong results if one only rest on this photometry alone. As for the cluster age, the isochrone matching shown in their Fig. 5 is somewhat weak mainly because the cluster main sequence displays only 2 mag in *J*. On the contrary, our optical CMDs show a more robust fitting not only because of the larger magnitude range but also because our isochrone matching follows pretty well the bend of the cluster main sequence.

4.4. NGC 2660

The first detailed study of NGC 2660 was carried out by Hartwick and Hesser (1973) by means of *UBV*, *uvby* and Hβ photoelectric photometry and *BV* photographic photometry. Since then several authors have studied this cluster as reported in Table 5. It is noticeable that through the years different authors with different techniques converge to a same $E_{(B-V)}$ color excess and the distance within the usual errors. The exception is the very discrepant value of $d_{\odot} = 4.34$ kpc found by Hesser and Smith (1987) well above the mean of ~2.8 kpc. The situation is quite different in relation to the age of NGC 2660 that spans a range going from 0.7 to 1.7 Gyr from one author to another. Certainly, the critical point resides in the metal content of the cluster, a question that still remains open. Since the purpose of our investigation excludes investigation of the metal content in NGC 2660 we rest onto the recent papers of Sestito et al. (2006) and Bragaglia et al. (2008) that concluded this cluster is solar metal content.

Just for the sake of completeness we want to mention the most recent paper of Sandrelli et al. (1999) based on *UBVI* photometry who found a probable 30% population of binary stars in NGC 2660. Mølholt et al. (2006) detected a number of δ Scuti variable stars in this object. Mermilliod et al. (2008), in turn, included this cluster in their large survey for red giants in open clusters identifying six members.

The radial density profile of NGC 2660, right middle panel in Fig. 8, shows a strong star density covering a radius of 6 arcmin (2MASS data) that emerges above a quite flat star field. Our survey is therefore covering the very nuclear cluster zone. In Fig. 12 we show the CMDs V *vs* $(B-V)$, upper left panel, and the V *vs* $(U-B)$, upper right panel. The middle upper panel shows the $(U-B)$ *vs* $(B-V)$ TCD. The lower left panel is the V *vs* $(V-I)$ CMD and the lower right panel is the $(B-V)$ *vs* $(V-I)$ color-color diagram.

The TCD, like in Ruprecht 60, is very useful to give a reasonable approximation to the true color excess affecting NGC 2660, even if there are no blue-type stars. The best ZAMS shifting in the TCD is

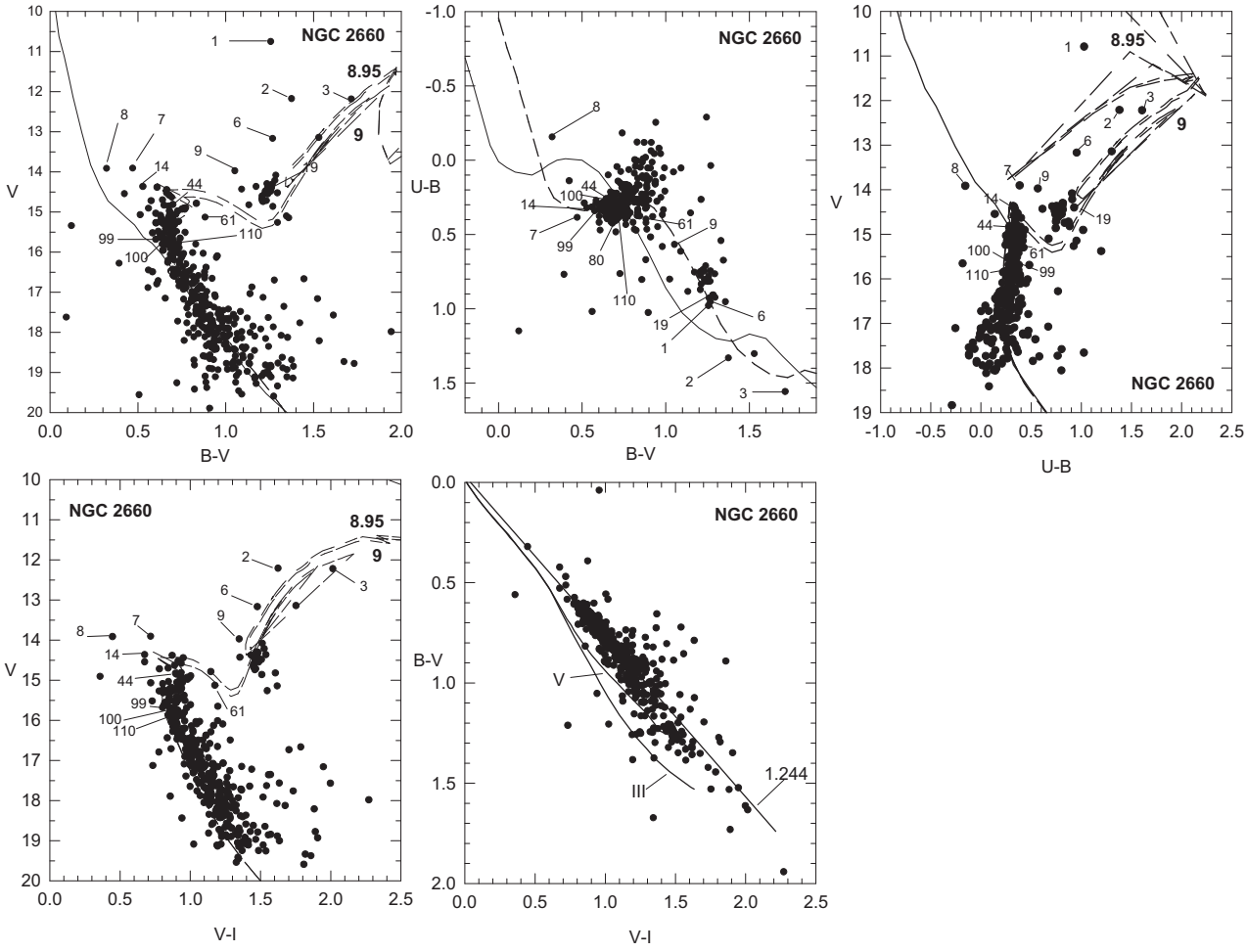

Fig. 12. Upper and lower panels as in Fig. 10. Idem for symbols and lines. The ZAMS in the TCD is shifted by a reddening $E_{(B-V)} = 0.33$.

for $E_{(B-V)} = 0.33 \pm 0.03$, a value slightly lesser than previous estimates reported in Table 5 but still in good agreement with the historical mean for NGC 2660. The CMDs show a very well populated cluster main sequence with a well defined turn-off. The data scatter along the main sequence seen in the V *vs* $B-V$ and V *vs* $(V-I)$ is relatively little what suggests, in our opinion, that contamination for field interlopers is low.

In the V *vs* $(B-V)$ and V *vs* $(V-I)$ CMDs of Fig. 8 we show the ZAMS of SK82 fitted with an apparent distance modulus $V - M_V = 13.25 \pm 0.15$ and the above mentioned $E_{(B-V)}$. Since the $(B-V)$ *vs* $(V-I)$ color-color diagram (lower right panel in Fig. 8) confirms that the absorption law $R = 3.1$ is completely valid in this region the absorption free distance modulus is $V_0 - M_V = 12.2 \pm 0.15$ that places NGC 2660 at a distance $d_\odot = 2.7 \pm 0.25$ kpc. This value agrees with those found in the literature (see Table 5).

A dominant feature in all the CMDs of NGC 2660 is the compact red clump at $V \sim 14.5$, also noticeable in the TCD at $(B-V) \sim 1.25$ and $(U-B) \sim 0.8$. Adopting the same temperament as in the case of the turn-off point of Ruprecht 60 we proceed to estimate the age of the cluster looking for the best set of isochrones embracing not only the turn-off point stars but also the evident red clump. Again, assuming the cluster's metallicity is solar, and by making use of Girardi et al. (2000) set of isochrones, we find that the best fit corresponds to the age interval $8.95 \leqslant \log(t) \leqslant 9$. Particularly good is the isochrones fitting in the V *vs* $(U-B)$ CMD. Notwithstanding, the red clump of this cluster raises some controversy since we could only fit simultaneously the cluster turn-off and the red clump stars in the V *vs* $(V-I)$ CMD. In the other two CMDs we note the clump looks blue-shifted and becomes impossible to fit for an isochrone. This effect has been noticed too in earlier works and that raised the controversy about the metal content of stars in this cluster. Photometry is unable to resolve the controversy. Just for the sake of curiosity we have made several attempts using different metal content isochrones without achieving a satisfactory result. Clearly a profound spectroscopic analysis is needed in NGC 2660.

MK types for stars in this cluster reported in Table 4 are illustrative in terms of comparing reddening and distance derived from photometry with the same data from spectroscopy alone. Data in Table 4 shows $E_{(B-V)}$ values ranging from 0.18 to 0.72 (only one star with this extreme value) while most stars have reddening values near the mean of 0.33. Looking at individual star distances with MK types in NGC 2660, we conclude that most of them are in front of the cluster at more than 0.5 kpc from it. These stars are 2, 3, 6, 9, 14, 19, 44, 80, 100 and 110. Photometric arguments (the location of these stars in the photometric diagrams in Fig. 12) favor that a number of them are not members directly or have low chances to be related to the cluster. Two stars, 8 and 61 are farther than the cluster distance; the star 61 is otherwise bad located in the photometric diagrams. We draw the attention to star 8, a B8III placed at a distance $d_\odot \sim 5.7$ kpc. We will return to this star in the next section. Star 1 has a chance, from a spectroscopic point of view, to be a likely member; however, its position in the photometric diagrams excludes it. Stars 99 and 7 are relatively close to

the cluster distance. In the case of star 7, and given its location near the turn-off, it becomes a potential blue straggler star. Like in Ruprecht 47 a large number of stars with MK types turned out to be non members. This fact permits us to throw away field interlopers with confidence and get clean diagrams of the cluster. There is no influence of interlopers on the cluster parameters since these latter depend on the turn-off location and the red clump. There is no influence of interlopers on the cluster parameters since these latter rely on the location of the turn-off and the red clump.

4.5. NGC 2910

Available information in the literature suggests NGC 2910 is a young open cluster. It has been previously studied by Becker (1960), Topaktas (1981), Ramsay and Pollaco (1992) and Kharchenko et al. (2005). Becker and Topaktas made use of the same data set (the Becker (1960) one) founding a large number of members amongst the bright stars in the zone. However, the deeper CCD photometric survey carried out by Ramsay and Pollaco (1992), Ramsay and Pollacco (1994) could only find 12 members. Kharchenko et al. (2005) revisited this cluster finding only 9 probable members. Evidently there are difficulties in understanding the upper main sequence of NGC 2910 that could be easily solved by undertaking a vigorous spectroscopic program. Although we have few stars with spectroscopy in this cluster we hope we can improve the knowledge of the region as we show below.

Despite our photometric survey includes a large portion of the cluster surface it is still insufficient to cover the entire cluster given its radial extension (see Fig. 4 lower panel). Photometric diagrams in Fig. 13 show an extended cluster main sequence down to $V \sim 17$ mag with very low scatter around the mean location. Contamination by field interlopers is not dramatic and the cluster appears clean against the star background. As for the cluster main sequence it appears affected by a uniform reddening value that we estimate $E_{(B-V)} = 0.22 \pm 0.01$ and show in Fig. 13 middle upper panel. This value disagrees with previous reports found in the literature and indicated in Table 5. Our reddening is more than twice the found for some authors but Kharchenko et al. (2005) who found $E_{(B-V)} = 0.34$ quite unrealistic from the TCD in the middle upper panel in Fig. 13.

We applied the same procedures used in the other clusters in this sample to derive the corresponding distance. The superposition of the SK82 ZAMS in the V *vs* $(B-V)$ and V *vs* $(U-B)$ CMDs has been done for a distance modulus $V - M_V = 11.22 \pm 0.15$. After correcting for visual absorption, taking into account that the extinction law is the standard one (see Fig. 13, lower right panel), the distance of NGC 2910 from the Sun turns out to be 1.3 ± 0.1 kpc a coincident value with earlier findings. Again we have a large discrepancy with Kharchenko et al. (2005) who found 2.6 kpc.

As for the age of the cluster we find a single isochrone able to fit the entire main sequence. This is the $\log(t) = 7.8$ for an age of 63 Myr. That is, from our data analysis, the cluster is a little bit older than earlier estimates.

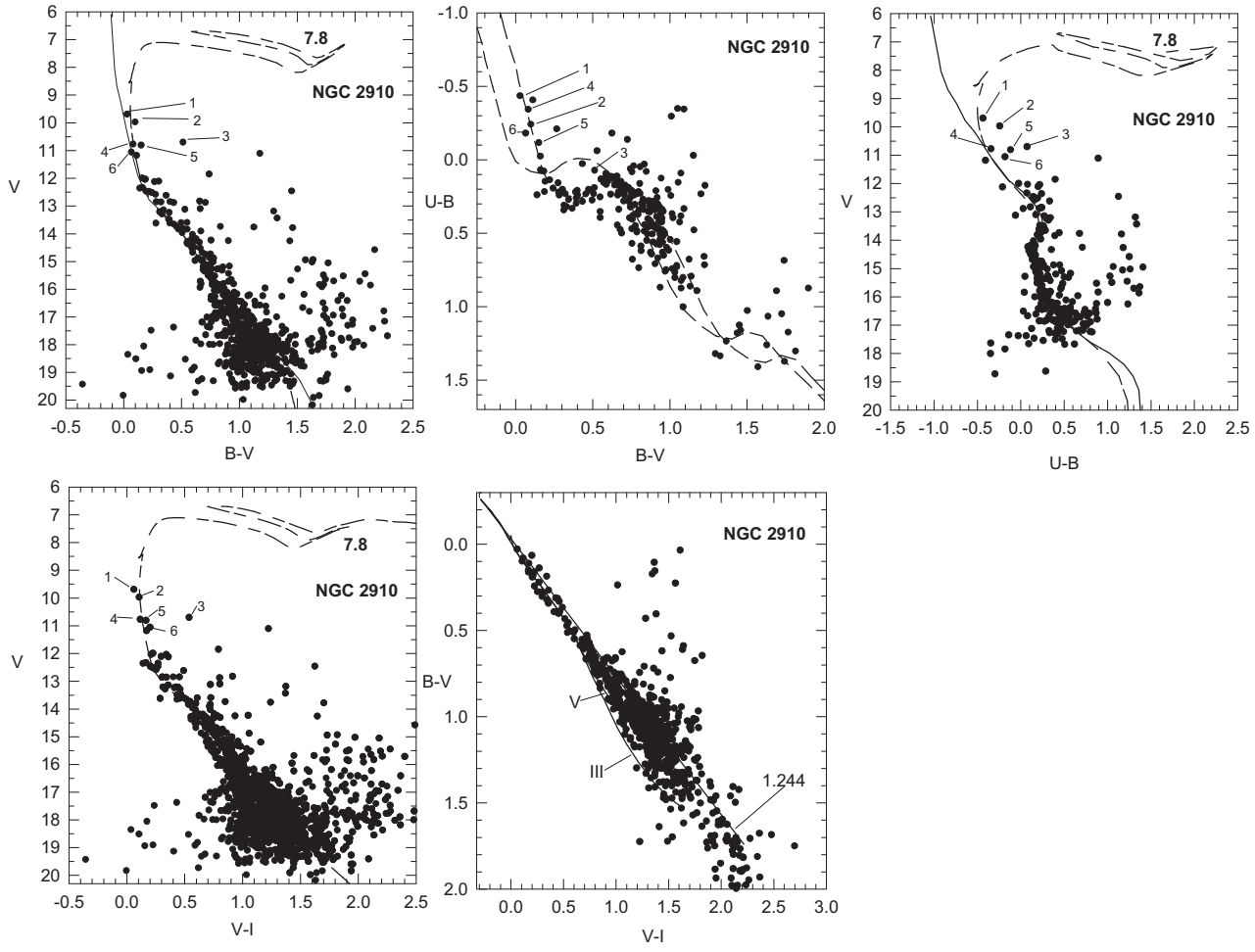

Fig. 13. Upper and lower panels as in Fig. 10. Idem for symbols and lines. The ZAMS in the TCD is shifted by a reddening $E_{(B-V)} = 0.22$.

MK types for NGC 2910 in Table 4 leave only three stars with chances to be cluster members; they are stars 1 and 2 of evolved B-Types and star 6, another B-type star. The other two stars, 4 and 5 in our notation, are not members of the cluster. They are too of B-types, one of late B-type and the other is a peculiar B-type star. The remaining star with MK-types in NGC 2910 is a background F-type star.

4.6. Reddening path

We finally show in Fig. 14 the path of $E_{(B-V)}$ against the distance for all the stars and clusters in the present sample. The upper panel includes stars with MK types in the field of clusters Ruprecht 20 and in Ruprecht 47. The position of Ruprecht 47 is indicated. In the lower panel we do the same for Ruprecht 60 NGC 2660 and NGC 2910. Following well known relations that state that $E_{(b-y)} = 0.7E_{(B-V)}$ we compare our reddening estimations with the findings of Kaltcheva and Hilditch (2000). For both regions under analysis, $240^\circ \leqslant l \leqslant 250^\circ$ and $264^\circ \leqslant l \leqslant 275^\circ$ the reddening values are entirely in agreement. The presence of some patches of dust may be responsible for the couple of nearby stars in Fig. 14, in both zones, showing high reddening values. Ruprecht 20 and Ruprecht 47 stars show different reddening behavior probably due to the fact that Ruprecht 47 is located along the Galactic plane (steadily increasing) while Ruprecht 20 is at more than 5 degrees below the plane (quite flat).

5. The Galaxy structure toward the Vela Gum

One of the clusters in our sample is Ruprecht 20 that we have already shown it is not a physical entity. This object is projected against the north of the Vela Gum in a region also known as Puppis association. The other cluster in our survey also in Puppis is Ruprecht 47 (in the limit with Pyxis constellation). Puppis is an intricate zone with a stellar structure hard to elucidate. Humphreys (1978) found various components of what is designated as Puppis OB1 association at 2.5 kpc from the Sun, while Havlen (1976) had, a little before, reported a second, more distant association, Puppis OB2 at 4.3 kpc. However, the existence of these two separate associations have been questioned by Kaltcheva and Hilditch (2000), who could not find evidences of them. Actually, these authors suggested the presence in the same Galaxy direction of two other star groups (at 1 kpc the first, and 3.2 kpc the second), but significantly lower in latitude, at $b \sim -4.0^\circ$. These two young star groups would surround, in projection, the star cluster NGC 2439, located at 3.5–4.5 kpc from the Sun (see Fig. 6 in Kaltcheva and Hilditch (2000)). Ruprecht 20 is situated a little below this last location and we found two stars, numbers 10 and 3 in our notation, of B8V and B9V spectral types in the field of this object at distances of ∼2.5 and ∼2.0 kpc respectively. Within distance errors of the order of 15%–20% as indicated in Section 3.3 these stars are placed in front of the stellar aggregate 2 proposed by Kaltcheva and Hilditch (2000) making this stellar group a long structure extending from 2 to 4 kpc from the Sun.

Ruprecht 47 is placed well along the Galactic plane at a distance $d_\odot = 4.4$ kpc. It becomes therefore clearly coincident with Puppis OB2 at 4.3 kpc according to Havlen (1976) assertion and the genetic connection with Puppis OB2 is supported by its age (less than 100 Myr). It is to mention that not far from the position of Ruprecht 47 there exists the open cluster Haffner 20 (246.97°, −0.93°) with similar age (Carraro et al., 2015) and at a distance of 5.5 kpc in the conjunction with the Perseus Arm. It seems, therefore, that Puppis OB2 may extend farther, even much more than previously indicated in the literature. Table 4 informs as well the existence of two B-type stars in the field of Ruprecht 47, one B1V and the other B5Ve at distances of 2.0 and 2.2 kpc respectively. If we follow the Humphreys (1978) discussion these two stars belong to Puppis OB1. Connecting our findings with those of Kaltcheva and Hilditch (2000) it seems that early type stars in Puppis constellation, including Puppis OB1 and OB2 and regions 1 and 2 from Kaltcheva & Hilditch compose a sort of thickening (maybe a bridge) of the Galactic disk of about 300 pc at 2–3 kpc from the Sun extending outward up to 6 kpc.

In the background of Ruprecht 47 there is another star, number 10 in our notation and classified B1V, placed at the huge distance of $d_\odot = 9.5$ kpc. This is a surprising finding since this distance implies we have detected a young stellar component of the innermost side of the Outer Arm. This star is very distant no matter the data set adopted. Indeed if we compute its spectroscopic parallax with data from Vogt and Moffat (1972) the distance from the Sun would be of the order of 10 kpc.

NGC 2660 and NGC 2910 are two clusters placed in the Vel OB1 association. According to Humphreys (1978) the nucleus of the association is placed at 1.8 kpc from the Sun. The cluster NGC 2660 is not subject of a discussion of this type in terms of its belonging to Vel OB1 since the age, around 1 Gyr, excludes it. However, there is another star, 8 in our notation, classified B8III and placed at ∼5.7 kpc from the Sun. We discuss below the

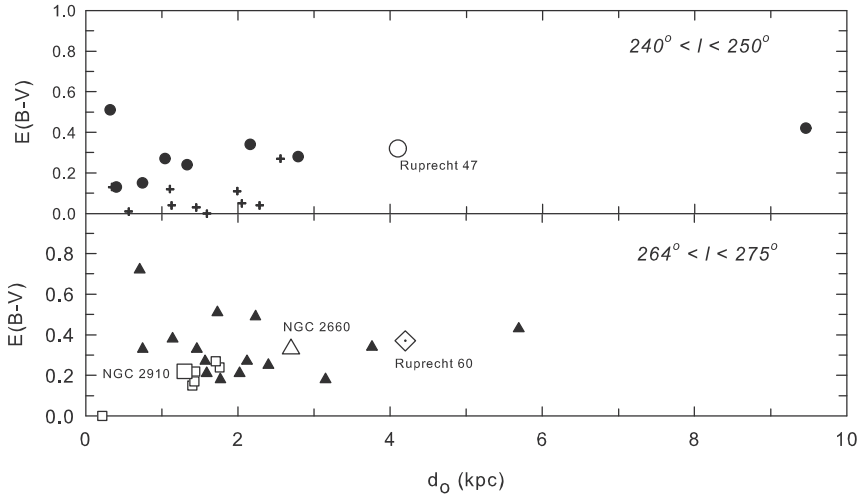

Fig. 14. The path of $E_{(B-V)}$ against distance from the Sun. The upper panel includes stars in Ruprecht 20, crosses, stars in Ruprecht 47 are indicated by small dots, large open circle gives the position of the cluster Ruprecht 47. Lower panel includes NGC 2910, big open square; small open squares indicate stars in the area of NGC 2910. Triangles are for stars in NGC 2660 while the big open triangle is the cluster NGC 2660. Open diamond gives the location of Ruprecht 60.

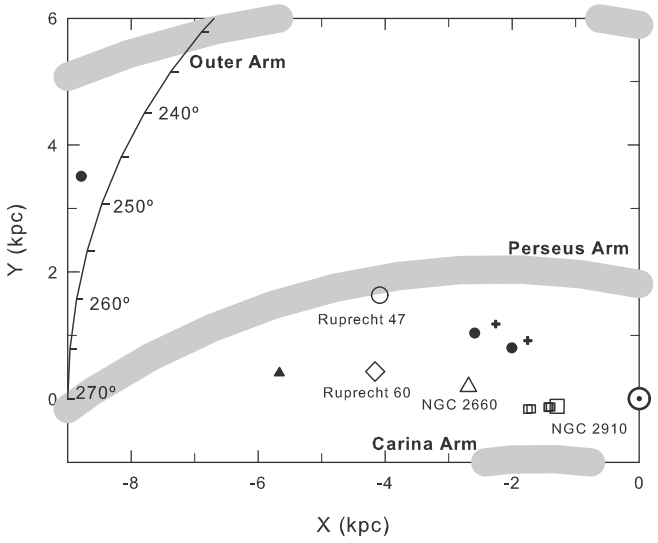

Fig. 15. X–Y projection onto the TGQ of blue stars and clusters in the present study. Symbols as in Fig. 14. The Sun is at 0, 0 (circle with a dot inside). The trace of the Perseus, Carina and Outer Arms (Vallée, 2005) are shown. The scale indicates the Galactic longitudes.

meaning of this star. As for NGC 2910, its distance of 1.3 kpc makes it a sure member of the Vel OB1 association and therefore a member of the Local Arm. In the cluster field there are also two stars, 4 and 5, B5Vp and B7III, at $\sim$ 1.7 kpc from the Sun respectively, that are likely members of the Vela OB1 association.

Fig. 15 is the X–Y projection of the TGQ showing the position of clusters and young stars analyzed in the present study. The picture in Fig. 15 is complementary of similar ones we have recently shown in Carraro et al. (2015) and enlarges the available information by including more clusters and stars in Puppis and Vela associations. Our Fig. 15 and Figs. 1 and 12 in Carraro et al. (2015) show the presence of a large number of blue stars and several young clusters composing a sort of bridge between the Perseus Arm and the Sun position covering from $\sim 220^\circ$ to $\sim 275^\circ$ in Galactic longitude. That is, the young stellar population we have found with spectroscopy forms part of the Local Arm in the TGQ, strictly speaking in Vela and Puppis associations. NGC 2910 is a young object member of the Local Arm and close to the border of the third and fourth Galactic quadrants. Probably this cluster is one of the farthest member of the Local Arm in the direction to Vela. The cluster Ruprecht 47 is also young and is placed close to the formal Galactic plane. So, we understand that this object is a likely member of the Perseus Arm (or a very distant member of Puppis OB2 in the Local Arm). As for the blue star, number 8, in the background of NGC 2660 it may be a member of the Local Arm though it is still possible for it to become one of the innermost members of the Perseus Arm. Fig. 15 shows the location of another remote blue star, number 10, seen in the background of Ruprecht 47 at 9.5 kpc from the Sun. We have already commented above that this star may become member of the innermost part of the Outer Arm. Nevertheless, what makes this object a singular star is its location along the Galactic plane. In fact, at $l = 240^\circ$—250° the warp is quite pronounced (Vázquez et al., 2008) but some young open clusters as Haffner 18 and Haffner 19 and blue stars in the background of Haffner 21 and Trumpler 9 can be found (see Carraro et al., 2015). Gathering all this information we interpret that the presence of this very remote young star in the Galactic plane is not an isolated fact but it is a strong indication that the Galactic thin disk is not only warped, but also flared, like the thick disk. Quite recently, Xu et al. (2013) have presented evidences of a large number of star formation regions with trigonometric parallaxes that extend the Local Arm back to the First Galactic Quadrant. Xu et al. (2013) stated also a series of questions (not answered yet) concerning the interpretation of the Local Arm: 1.- it is a branch of the Perseus Arm, 2.- it is part of a major arm or 3.- it is an independent spiral arm segment. Unfortunately, we cannot speculate about the nature of the Local Arm because our observations were designed just to establish the existence and the spatial distribution of young objects in the TGQ. More observations (photometry and spectroscopy) for a precise estimation of cluster parameters are needed in order to reach a plausible answer to these questions from an optical point of view. Meanwhile, a comparison of our Fig. 15 with their Fig. 10 reveals that our findings are in good agreement with theirs in terms of the distribution of young population throughout the Local Arm in TGQ.

6. Conclusions

We presented in this article the results of a photometric and spectroscopic survey carried out in five cluster located at $240^\circ < l < 275^\circ$ and $0^\circ > b > -6^\circ$. This region comprises mostly the Vela Gum region and includes part of the Puppis association.

One of our clusters, Ruprecht 60, has been studied with *UBV* photometry for the first time and its parameters are now improved. Other of the clusters, Ruprecht 20, is not a cluster since neither from star counts used to construct its radial density profile nor from the photometric diagrams we can conclude that it is a true entity. It is just a random stellar fluctuation.

For the other three clusters, Ruprecht 47, NGC 2660 and NGC 2910 we have improved also their parameters.

From the point of view of identification of large stellar structures in this portion of the Galaxy we have found evidences that favor the presence in Puppis, at $b^\circ = -4$, of a sort of bridge connecting two regions defined by Kaltcheva and Hilditch (2000). Ruprecht 47 is definitely a member of Puppis OB2 and in its field we also found two blue stars related with Puppis OB1. NGC 2910 becomes member of Vel OB1 and also a couple of blue stars with no relation to NGC 2910.

Ruprecht 60 and NGC 2660 are too old objects with no genetic relation to the associations they are seen against.

As for two peculiar isolated stars we report the presence of a very distant star seen against the field of Ruprecht 47 placed at almost 10 kpc from the Sun. Ruprecht 47 is along the formal Galactic plane ($b^\circ = -0.188$) and this remote star in the background may belong to the innermost part of the Outer Arm. Another interesting star has been found in the field of NGC 2660 at near 5.7 kpc from the Sun. This star could be member of the innermost part of the Perseus Arm or a far member of the Local Arm. As for the grand design structures in the TGQ we are in the position to confirm the angular extension of the Local Arm from 220° to 275°. Our findings are in good agreement with previous studies (see Carraro et al., 2015) we have already performed in the sense that our evidences indicate that the Galactic plane is not only warped but also flared. This is, thin disk population shows a pattern similar to the shown by the thick disk. Moreover, there is a good spatial agreement with Xu et al. (2013) findings. Finally, the kind of observations we performed do not allow to speculate about the nature of the Local Arm but our evidences -collected in several papers as indicated in Section 1 and concerning strictly the TGQ- suggest that the Local Arm may even cross the Perseus Arm and reach the Outer Arm.

Acknowledgments

We warmly acknowledge the CASLEO staff for the very professional support along the years. One of us, RAV, wishes to thank to Dr. Garrison for the allocation of observing time at the University of Toronto Southern Observatory in Las Campanas Observatory, Chile. EG, GS and RAV thank the financial support from CONICET PIPs 1359 and 5970 and from La Plata Observatory. We especially acknowledge to our anonymous referee for the careful and collaborative report that greatly contributed to improve the value of our manuscript. This publication makes use of the Two Micron All Sky Survey, which is a joint project of the University of Massachusetts and the Infrared Processing and Analysis Center/California Institute of Technology, funded by the National Aeronautics and Space Administration and the National Science Foundation. The Digitized Sky Survey was produced at the Space Telescope Science Institute under U.S. Government grant NAG W-2166. The images of these surveys are based on photographic data obtained using the Oschin Schmidt Telescope on Palomar Mountain and the UK Schmidt Telescope. The plates were processed into the present compressed digital form with the permission of these institutions.

References

Aarseth, S.J., 1996. In: Milone, E.F., Mermilliod, J.-C. (Eds.). The Origins, Evolution, and Destinies of Binary Stars in Clusters. ASP Conf. Ser., 90, 423.
Becker, W., 1960. Z. Astrophys. 51, 49.
Bonatto, C., Bica, E., 2010. MNRAS 407, 1728.
Bragaglia, A., Sestito, P., Villanova, S., Carreta, E., Randich, S., Tosi, M., 2008. VizieR On-line Data Catalog.
Burton, W.B., te Lintel Hekkert, P., 1986. A&AS 65, 427.
Carraro, G., Vázquez, R.A., Moitinho, A., Baume, G., 2005. ApJ 630, L153.
Carraro, G., Moitinho, A., Zoccali, M., Vázquez, R.A., Baume, G., 2007. AJ 133, 1058.
Carraro, G., Vázquez, R.A., Costa, E., Ahumada, J.A., Giorgi, E.E., 2015. AJ 149, 12.
Choi, Y.K., Hachisuka, K., Reid, M.J., Xu, Y., Brunthaler, A., Menten, K.M., Dame, T.M., 2014. ApJ 790, 99.
Churchwell, E., Babler, B.L., Meade, M.R., Whitney, B.A., Benjamin, R., Indebetouw, R., et al., 2009. PASP 121, 213.
Clariá, J.J., 1974. AJ 79, 1022.
Cousins, A.W.J., 1978. MNSSA 37, 62.
Dame, T.M., Hartmann, D., Thaddeus, P., 2001. ApJ 547, 792.
Dean, J.F., Warren, P.R., Cousins, A.W.J., 1978. Dean 183, 569.
de La Fuente Marcos, R., 1997. A&A 322, 764.
Efremov, Y.N., 1998. Astron. Astrophy. Trans. 15, 3.
Fitzgerald, M.P., 1968. AJ 73, 983.
Frandsen, S., Dreyer, P., Kjeldsen, H., 1989. A&A 215, 287.
Friel, e.d., 1995. ARA&A 33, 381.
Geisler, D., Clariá, J.J., Minniti, D., 1992. AJ 104, 1892.
Georgelin, Y.M., Georgelin, Y.P., 1976. A&A 49, 57.
Giorgi, E.E., Vázquez, R.A., Solivella, G.R., Orellana, R.B., Nuñez, J., 2007. New Astron. 12, 461.
Girardi, L., Bressan, A., Bertelli, G., Chiosi, C., 2000. A&AS 141, 371.
Grotues, H.-G., Gocherman, J., 1992. The Messenger 68, 43.
Hartwick, F.D.A., Hesser, J.E., 1973. ApJ 183, 883.
Havlen, R.J., 1976. A&A 47, 193.
Henderson, A.P., Jackson, P.D., Kerr, F.J., 1982. ApJ 263, 116.
Hesser, J.E., Smith, G.H., 1987. Publ. Astron. Soc. Pac. 99, 1044.
Hou, L.G., Han, J.L., 2014. A&A 569, 125.
Hou, L.G., Han, J.L., Shi, W.B., 2009. A&A 499, 473.
Humphreys, R.M., 1978. ApJS 38, 309.
Kaltcheva, N.T., Hilditch, R.W., 2000. MNRAS 312, 753.
Kharchenko, N.V., Piskunov, A.E., Roser, S., Schilbach, E., Scholz, R.D., 2005. A&A 438, 1163.
Kim, J.S., Walter, F.M., Wolk, S.J., 2005. ApJ 129, 1564.
King, I., 1962. AJ 67, 471.
Kroupa, P., Aarseth, S., Hurley, J., 2001. MNRAS 321, 699.
Kulkarni, S.R., Heiles, C., Blitz, L., 1982. ApJ 259, L63.
Landolt, A.U., 1992. AJ 104, 340.
Lyngä, G., 1987. Catalog of Open Cluster data, Strasbourg: Centre de Donnees Stellaires. (fifth ed.).
May, J., Murphy, D.C., Thaddeus, P., 1988. A&As 73, 51.
May, J., Alvarez, H., Bronfman, L., 1997. A&A 327, 325.
McCarthy, C.C., Miller, E.W., 1974. AJ 79, 1396.
Mermilliod, J.-C., Mayor, M., Udry, S., 2008. A&A 485, 303.
Meynet, G., Mermilliod, J.-C., Maeder, A., 1993. A&AS 98, 477.
Milone, A.A.E., 1992. PASP 104, 1268.
Moffat, A.F.J., FitzGerald, M.P., 1974. A&A 34, 291.
Moffat, A.F.J., Vogt, N., 1973. A&A 23, 317.
Moitinho, A., 2001. A&A 370, 436.
Moitinho, A., Vázquez, R.A., Carraro, G., Baume, G., Giorgi, E.E., Lyra, W., 2006. MNRAS 368, L77.
Mølholt, T.E., Frandsen, S., Grundahll, F., Glowienka, L., 2006. Commun. Asteroseismology 148, 12.
Murphy, D.C., May, J., 1991. A&A 247, 202.
Nakanishi, H., Sofue, Y., 1991. PASPJ 55, 191.
Perren, G., Vázquez, R.A., Carraro, G., 2012. A&A 548, 125.
Ramsay, G. Pollacco, D.L., 1994, A&As V. 104.
Ramsay, G., Pollaco, D.L., 1992. A&As 94, 73.
Reed, B.C., 1989. A&AS 77, 447.
Reed, B.C., 1990. AJ 100, 737.
Reed, B.C., FitzGerald, P.M., 1984. MNRAS 211, 235.
Reed, B.C., FitzGerald, P.M., 1984. MNRAS 211, 243.
Reed, B.C., FitzGerald, P.M., 1985. MNRAS 212, 987.
Reid, M.J., Menten, K.M., Zheng, X.W., Brunthaler, A., Moscadelli, L., Xu, Y., Zhang, B., et al., 2009. AJ 700, 137.
Reid, M.J., Menten, K.M., Brunthaler, A., Zheng, X.W., Dame, T.M., Xu, Y., Wu, Y., et al., 2014. ApJ 783, 130.
Russeil, D., 2003. A&A 397, 133.
Sahu, M.S., 1992 (Ph.D. thesis). University of Groningen.
Sandrelli, S., Bragaglia, A., Tosi, M., Marconi, G., 1999. MNRAS 309, 739.
Schlegel, D.J., Finkbeiner, D.P., Davis, M., 1998. ApJ 500, 525.
Schmidt-Kaler, T., 1982. Landolt-Börnstein, Group VI. Stars and Star Clusters, vol. 2b. Springer, Berlin (p. 15).
Sestito, P., Bragaglia, A., Randich, S., Carretta, E., Prisinzano, L., Tosi, M., 2006. A&A 458, 121.
Slawson, R.W., Reed, B.C., 1988. AJ 96, 988.
Stetson, P.B., 1987. PASP 99, 181.
Topaktas, L., 1981. A&AS 45, 111.
Vallée, J.P., 2005. AJ 130, 569.
Vallée, J.P., 2013. Int. J. A&A 3, 20.
Vallée, J.P., 2014. MNRAS 442, 2298.
Vázquez, R.A., Feinstein, A., 1990. A&AS 86, 209.
Vázquez, R.A., Baume, G., Feinstein, A., Prado, P., 1994. A&AS 106..3, 39.
Vázquez, R.A., May, J., Carraro, G., Bronfman, L., Moitinho, A., Baume, G., 2008. ApJ 672, 930.
Vogt, N., Moffat, A.F.J., 1972. A&ASS 7, 133.
Vogt, N., Moffat, A.F.J., 1975. A&AS 20, 85.
Wouterloot, J.G.A., Brand, J., Burton, W.B., Kwee, K.K., 1990. A&A 230, 21.
Wu, Y.W., Sato, M., Reid, M.J., Moscadelli, L., Zhang, B., Xu, Y., Brunthaler, A., Menten, K.M., Dame, T.M., Zheng, X.W., 2014. A&A 566, 17.
Xu, Y., Li, J.J., Reid, M.J., Menten, K.M., Zheng, X.W., Brunthaler, A., Moscadelli, L., Dame, T.M., Zhang, B., 2013. ApJ 769, 15.